MASTER'S DEGREE THESIS

Master of Science in Advanced Mathematics and Mathematical Engineering

Title: Phase response to stimuli: the case of excitable systems

Author: Román Moreno González

Advisor: Antoni Guillamon

Department: Mathematics UPC

Academic year: 2018-2019

UNIVERSITAT POLITÈCNICA DE CATALUNYA
BARCELONATECH
Facultat de Matemàtiques i Estadística

Universitat Politècnica de Catalunya
Facultat de Matemàtiques i Estadística

Master in Advanced Mathematics and Mathematical Engineering

Master's thesis

Phase response to stimuli: the case of excitable systems

Román Moreno González

Supervised by Antoni Guillamon Grabolosa

June, 2019

I would like to thank my supervisor, Antoni Guillamon, for his enthusiasm, continuous support, his patience and for his valuable advice and thorough feedback during these months. Without his guidance this thesis would by no means have been possible.

In addition, my most sincere thanks to the Barcelona Graduate School of Mathematics for giving me the chance to participate in the Maria de Maeztu Master Internships Programme 2019. It has been a very valuable support as well as a big source of motivation.

Finally, I would like to thank my closest family. To my mother María Teresa, my father José Ignacio and my brother, Ignacio: thank you for being so comprehensive and supportive when my motivation was not at its peak and for your kind encouraging words. Also, many thanks to my cousin, Daniel, who, as a young researcher, has shared with me many enlightening experiences and thoughts.

Abstract

Phase response analysis is a useful tool for describing how perturbations affect oscillatory systems. Computation of phase resetting curves for oscillatory systems is a well known problem, and different tools are available, including numerical methods or more analytic techniques such as the adjoint method. The concept of PRF has also been extended to the more general phase resetting functions, thus allowing to evaluate the effect of stimuli applied under more general conditions. In this thesis our main goal is to extend these ideas to the case of excitable systems where there are no sustained oscillations. We use theoretical results to justify the definition of an asymptotic phase and use normal form transformations for the computations. Finally, we apply the method to two simple example and examine the results for several sets of parameters.

Keywords

Phase resetting curve, phase resetting function, excitable cells, neuron models, isochronicity, isochrons, strong focus, asymptotic phase.

Contents

1. Introduction

Mathematical models in neuroscience usually include systems of ordinary differential equations that reproduce the oscillatory behaviour of neurons. An interesting question in neuroscience is how neurons or networks of neurons react when we apply stimuli on them: we can ask whether a high enough stimulus will produce oscillations or what effect it will have in the oscillatory phase. The latter appears in the biological context of electrical stimulation of spiking neurons and is referred to as phase response analysis. Phase response analysis has already been studied for oscillatory systems: the effect of perturbations in an oscillatory state is well known both experimentally and theoretically. Its mathematical description is the phase resetting curve, which can be computed both experimentally, by actually perturbing the neuron and observing the advancement or delay of the oscillation peak, and theoretically. A classical theoretical approach to perturbations on the oscillating systems is the adjoint method, which outputs phase response curves as a solution of a differential equation. Further studies have recently characterized the effect on phase of perturbations in oscillatory regimes for systems that have not reached the stable oscillation by extending the phase concept by means of the asymptotic phase and expressing the system dynamics in a simplified way.

The goal of this work is to extend this phase response treatment and characterize the response of excitable neuron to stimuli. Ultimately we would like to study the phase response to stimuli for several values of a parameter that causes the system to go through a bifurcation, thus relating the excitable state response to the oscillatory response. As a first step we need to extend the concept of asymptotic phase to the dynamics governed by an attractive focus. This allows to use concepts and techniques already known in studies of oscillatory systems, such as Phase Resetting Curves (PRC), Phase Resetting Functions (PRF) and isochrons.

Our main approach is to take advantage of normal form theory and the fact that the dynamics of excitable cells is linearizable by a change of variables. By explicitly computing this change of variables we intend to compute isochrons and phase resetting functions in the linear and well known case and to bring this result back to the nonlinear case using the appropriate change of coordinates. Once we have established a procedure for this computation, we apply it to low-dimensional cases and simple networks: we consider reduced systems with one gating variable and self-excited reduced systems.

In section 2 we present the basic concepts used for modelling neurons, such as the electrical analogue for modelling potential variations, gating variables and synaptic currents models, as well as some key concepts as excitable or oscillatory state. This provides a context to, in section 3, lay out the concepts of phase and asymptotic phase that play a very important role throughout the thesis. In that section we also state more formally the problem we want to analyze and present some theoretical background to tackle it. Section 4 is devoted to explaining how to apply in practice the methods presented in the previous sections. Finally, in section 5 we perform the calculations for two specific systems: the self-excited neuron, and the Fitzhugh Nagumo model. We vary the model parameters and comment on whether these variations have an impact on the results obtained and, if so, in what way.

2. Modelling of neurons

The main variable defining a neuron's activity is its membrane potential, represented by V, defined as the voltage difference between the exterior and the interior of the cell membrane. The potential is a time-dependent variable that evolves according to many factors in a complex way: external electric stimuli, synaptic connection to other cells and internal cell dynamics governed by electrochemical forces. We usually model neurons with an autonomous dynamical system defined in a phase space whose dimension depends on the complexity of the model we choose. The general equation looks like:

$$\dot{\mathbf{x}} = X(\mathbf{x}), \tag{1}$$

where the first component is the voltage $\mathbf{x(t)} = (V(t), ...) \in \mathbb{R}^n$. The field X can become incredibly complex as we include more variables. In this section we are going to present the simplest model — that fails to capture the essential feature of the neurons, namely spiking — but which displays some of the elements generally used; as well as the most extended Hodgkin-Huxley model.

2.1 Passive membrane

Biologically, a neuron is a complex system surrounded by a membrane that delimits an exterior and an interior, where the potential difference V occurs. What determines the electrical behavior of a neuron is the presence of **charged ions** and **their flow in and out of the membrane**. The most commonly considered ions, due to their higher relevance, are K^+ and Na^+. These ions move through the membrane using **channels** that allow them to enter or exit the cell. Channels may be static if their opening status does not vary along time or dynamic if they do, thus contributing to the global dynamics of the cell. These two kinds of channels give rise to two notions when dealing with neuron modelling: **passive membrane** and **active membrane**.

Modelling a neuron using an equation of the type of (1) means to encode the changes of its voltage difference in a set of differential equations. The potential difference in neurons is caused by the presence and concentration differences of positive ions, mainly potassium K^+ and sodium Na^+. The difference in the total charge inside the neuron and outside it causes a non-zero potential difference. This difference evolves with time given that ions can flow through the membrane in or out of the cell. From a physical point of view the flow of ions occurs in order to bring the cell to the equilibrium, which is twofold:

- As chemical substances, the concentrations inside and outside tend to be equal.
- As electrical charges, they tend to counteract potential differences.

As a result, an unperturbed neuron is not at 0V: it is at the so-called **resting potential**, that is, the potential generated by the concentrations that minimize both the chemical and the electrical forces.

This value is not necessarily zero given that the neuron equilibrium is an electrochemical equilibrium, so there has to be an electrical force to counteract chemical forces. The classical approach to modelling electrical dynamics of neurons is to assume that they behave like circuits: the membrane acts like a capacitor — a part of the circuit that stores electric charge — ; channels act as a resistance — they counteract electric current flow — ; and concentration gradients act as batteries — generating the electromotive force that generates the current flow.

We can encode these principles in an equation by applying the first of Kirchoff's laws: the intensity inflow and outflow has to add up to zero. The intensity of a capacitor of capacitance C is given by:

$$I_{\text{membrane}} = \frac{dQ}{dt} = C\frac{dV}{dt}\,. \tag{2}$$

Since the capacitor is the membrane, this current flux has to equal the current that goes through the ionic channels. For simplicity we can consider there is only one ionic channel and that the resting potential is V_0. Then, the intensity is related to the voltage difference via the **conductance**, g

$$I_{ion} = -g(V - V_r)\,. \tag{3}$$

Therefore, this simplified equation is:

$$C\frac{dV}{dt} = g(V - V_r)\,. \tag{4}$$

Equation (4) is called passive membrane model, since it considers the membrane does not play any role in the dynamics except for having a static capacity. Solving this equation we would see the voltage would evolve towards a fix value and no further dynamics could be observed. Indeed, we can see that equation (4) has an exponential solution tending to a resting state:

$$V(t) = V_r + (V_0 - V_r)e^{-g/C\cdot t}\,. \tag{5}$$

2.2 Voltage gated channels

The passive membrane model only produces potentials that tend exponentially to the resting value; however, biological experiments have shown that membrane voltage exhibit different kinds of behaviours according to the physical parameters of the cell. One of the most characteristic behaviours of membrane potential is the presence of spikes when a high enough stimulation is applied. Spikes are steep increases in voltage followed by a fast decrease which occur when exterior stimuli are intense enough under some circumstances. Hodgkin and Huxley where the first to identify the internal mechanism that caused this behaviour. They proposed that channels that allow the inflow and outflow of ions through the membrane are dynamic, that is, they adapt to the current state of the systems and vary along time. In equation (4) this would be equivalent to g being a function of time. The experimental confirmation to this fact came by means of the **voltage clamp**: an experimental electronic technique that keeps the membrane potential at rest, thus ensuring the experimenter that all measures of the variations of the voltage are due to factors other than the mere flux of electrons. Indeed, the experimentalists could attribute changes in the neuron voltage to the opening and closing of the ionic channels. Two of the main conclusions of these experiments were:

- K^+ channels only have activation phase: the higher the values the potential reaches, the wider the channel opens therefore increasing even more the channel conductance.
- Na^+ channels open sharply when the voltage begins to rise; however, for very high voltage values they close again, which suggests a **slow-paced deactivation mechanism**.

Mathematically, the gated channels are modelled as follows: the conductance for each ion is a time dependent function — $g_{Na}(t)$ and $g_K(t)$ — which evolves following a balance between the closing and opening channel. The expression of these time-dependent conductances consists of a maximum conductance scaled by a factor that represents *how open the channel is*. This factor can be thought of as the probability of a component of the channel being open. The probability of a channel opening and closing depends indirectly on time through its dependence on the voltage. Ionic channels conductance approaches exponentially a voltage-dependent value, given typically by a sigmoid-like function. Biological studies of the gated channels as well as the aforementioned conclusions of the clamp voltage experiment lead to models of the gating variables current using the general formulation

$$I_{ion} = g_{ion} m^a h^b (V - V_{ion}) \,, \tag{6}$$

where the voltage part is the difference between the membrane voltage and the **reversal potential**. The reversal potential is characteristic for each ion and is the potential at which the concentration gradient and the electrical force compensate and stop the flux of that ion through the membrane. The variables m and h take values between 0 and 1. The m (or another letter if there are several ions) represents the channel activation, whereas h represents the deactivation of the channel. The constants a and b are integers that account for the effect of m and h on the current, respectively, and they are related to the number of independent physical components in the channel. The channel is most widely open when $m = h = 1$, in which case the ionic current has its highest value, $I_{ion} = g_{ion}(V - V_{ion})$. In the Hodgkin-Huxley model we find the following ionic channels:

- One potassium gating variable: it is represented by n, and $a = 4$ since the channel opening depends on four independent components. Thus, the potassium channel is: $g_K(t) = g_K \cdot n(V)^4$.

- The sodium channel: m represents the opening of the channel and h represents the deactivation of the channel. In this case there are three independent components, so $a = 3$, whereas there is only one deactivating component, so $b = 1$. The sodium current is therefore $g_{Na}(t) = g_{Na} \cdot m(V)^3 \cdot h(V)$

Given that the probabilities m, n and h tend to the corresponding m_∞, n_∞ and h_∞ values, their dynamics are modelled by the equations:

$$\begin{cases} \dot{n} &= \frac{n - n_\infty(V)}{\tau_{\mathbf{n}}} \\ \dot{m} &= \frac{m - m_\infty(V)}{\tau_{\mathbf{m}}} \\ \dot{h} &= \frac{h - h_\infty(V)}{\tau_{\mathbf{h}}} \end{cases} . \tag{7}$$

The constants τ_n, τ_m and τ_h are time scales: if they are low, time derivatives are very high and therefore gating variables are almost equal to their steady-state values. If they are slow it is the other way round. The fact that h is considered to be a *deinactivation variable* comes from the qualitative difference between sodium and potassium channel behavior: the reason why the potassium channel is more complex than the sodium one is that **potassium conductance always increases with voltage**, so it is correctly modelled by the increasing n function; whereas **sodium conductance increases rapidly and decays slowly as voltage keeps increasing**. This suggests a deactivation occurs after the peak of the conductance has reached, and its negative effect has to outweigh that of the activation.

The complete Hodgkin-Huxley model is, therefore, as follows:

$$\begin{cases} C\dot{V} &= -\mathbf{g_{Na}}m^3h(V-V_{Na}) - \mathbf{g_K}n^4(V-V_K) - \mathbf{g_L}(V-V_L) + \mathbf{I_{app}} \\ \dot{n} &= \frac{n-n_\infty(V)}{\tau_\mathbf{n}} \\ \dot{m} &= \frac{n-n_\infty(V)}{\tau_\mathbf{m}} \\ \dot{h} &= \frac{h-h_\infty(V)}{\tau_\mathbf{h}} \end{cases} . \tag{8}$$

If we have two four-dimensional dynamical systems representing a neuron and we link them via a synapse we will end up with an eight-dimensional system. In order to simplify the system to be able to apply lower dimension techniques we can **simplify the gating variables** as well as **consider self excitation**. The first simplification implies that all the variables are reduced to one single channel that encapsulates all the chemical flux through the membrane. To justify this reduction we have to note the following: the dynamics of the gating variables consists of the time dependent variables tending to the time independent (but voltage dependent) *infinity values*, that is, the values at which, for the current voltage status, they would tend in an infinite time. All this process happens at a time given by the magnitude of the time *constant* τ. When the time constant is very low, the time derivatives are very high, which means the infinity status is reached very rapidly. In view of this, since τ_m is much higher than the other time constants, m can be interpreted to instantly reach the infinity value, so it can be replaced by the infinity value. On the other hand, there is an experimental relation between n and h which further reduces the system. This makes the system two dimensional and, together with the self-excitement, it keeps the self excited system at dimension two.

2.3 Action potential

Gating variables provide the necessary dynamics for the cell to exhibit **action potentials**. An action potential is a spike in the temporal profile of the voltage: a neuron in a resting state without any stimuli would remain there forever. Only when it is perturbed with an intense enough stimulus is it capable of spiking. The action potential can happen isolated or periodically, but essentially the underlying mechanism is the same. Since the resting state is usually a negative voltage, it is considered as a polarized state. An increase of the voltage from the negative resting value is referred to as depolarization (it brings the neuron closer to 0), whereas a decrease in the voltage value is referred to as hyperpolarization (it polarizes it even more). The schematic phases of the action potential are the following:

1. A stimulus increases the voltage.
2. The sodium gating variable opens quickly, so the inflow of sodium increases.
3. Potential rises (this is referred to as **depolarization)**.
4. The K^+ channel starts to open, so K^+ ions flow out, having a negative impact on the voltage.
5. The deactivation of the sodium channel starts: this goes in favor of hyperpolarization.
6. The opening of the potassium channel causes huge outflow of potassium: the voltage decreases.

2.4 Excitable and oscillatory regimes

The dynamical system that represents a neuron often presents two different behaviors: **excitable** or **oscillatory**. The excitable status is a set of parameters where the system presents an equilibrium point that represents the resting state of the cell. Since the resting state of the cell is the state it tends to when there are no stimuli, the eigenvalue of the linearization at this point has negative real part. That is, it is a point-attractor. On the other hand, the oscillatory state is the set of parameters where the system presents an attractive limit cycle and it represents biologically the periodic action potential the neuron exhibits when it is subject to a sufficiently high stimulation. This set of parameters usually includes higher values of the applied current: when the cell is excited with enough intensity it spikes periodically, and when the stimulation ceases it goes back to the equilibrium.

Mathematically, an excitable state is represented by a node or a focus: the system returns to the equilibrium with or without oscillations. In a two-dimensional system, the linearization is of the form:

$$\begin{pmatrix} \dot{x} \\ \dot{y} \end{pmatrix} = \begin{pmatrix} a & b \\ c & d \end{pmatrix} \begin{pmatrix} x \\ y \end{pmatrix}. \tag{9}$$

The eigenvalues in this case have a explicit formula:

$$p(\lambda) = (a-\lambda)(d-\lambda) - bc = \lambda^2 - (a+d)\lambda + ad - bd = 0 \implies \lambda = \frac{(a+d) \pm \sqrt{(a+d)^2 - 4(ad-bc)}}{2}.$$

So there is a focus when $(a+d) < 0$ and $4(ad-bc) > (a+d)^2$.

The excitable states are conceptualized as a potential oscillatory state, and are thus classified in regard to the kind of oscillation they can give rise to, according to **oscillation frequency** and **oscillation profile**.

- Type I: an excitable cell is said to be of type I if, when sufficiently stimulated, the following characteristics appear: oscillation occurs much later than stimulus; frequency appears at zero value and slowly increases, that is, frequency is a continuous function; and shape is less variable, regardless of the intensity of the stimulus. It is associated to a Saddle Node on Invariant Circle (SNIC) bifurcation, which qualitatively explains this behaviour: the invariant circle limits the shape of the peak, the saddle node makes the frequency be 0 at the moment the orbit appears, and it *slows down* the spiking, since it attracts the neuron for a long time before it finally spikes.
- Type II: an excitable cell is said to be of type I if, when sufficiently stimulated, oscillation frequencies start at a certain threshold. That is, if we consider the oscillatory frequency of a resting state is zero, the oscillation frequency is discontinuous. Another property is the fact that oscillations occur very shortly after the stimulus. As for the type of oscillation, their shape varies continuously according to the intensity of the stimulus. They are associated with a Hopf bifurcation.

The transition to the oscillatory regime represents mathematically a bifurcation, that is, a change in the global dynamics of the system caused by a change in one or several parameters. Let us briefly discuss the two bifurcations that are usually related to the two types of excitability:

- **Hopf bifurcation**: it occurs in systems of dimension at least 2 when the hypotheses for Hopf bifurcation theorem are met:

- There is a value of the parameter where the system has a pair of pure imaginary conjugate eigenvalues.
- The derivative of the real parts of the eigenvalue at the bifurcation point is not zero.
- An extra condition of the specific normal form properties of the system (which translates to a technical condition on the derivatives).

In this case the Hopf bifurcation theorem states that there is a smooth curve of equilibria and a surface of periodical orbits in the space $\mathbb{R}^n \times \mathbb{R}$, where the second factor corresponds to the parameter space. Qualitative, this means that when the system crosses the bifurcation value the equilibrium changes its stability giving rise to a limit cycle around it. This limit cycle, so to speak, *takes away* the stability of the point: a stable point turning into an unstable one will generate a stable limit cycle, and otherwise for unstable points turning stable. When the limit cycle is stable we refer to the bifurcation as **supercritial Hopf bifurcation**; otherwise we refer to it as **subcritical Hopf bifurcation**. This explains the non-existing delay between stimulus and oscillation: as soon as the system passes the threshold it starts to oscillate with a positive frequency.

- **Saddle node on a limit cycle bifurcation**: it occurs when two equilibrium points, one of them being a saddle point, connected by a heteroclinic orbit collide. For the parameter value where the collision occurs the heteroclinic orbit becomes a homoclinic orbit with infinite period — zero frequency. When the parameter is further modified the equilibrium point disappears and only the limit cycle, this time with finite period, appears. This process accounts for the fact that the frequency is a continuous function that starts at zero when the limit cycle is generated. The reminiscence of the attraction of the disappeared saddle-node produces a delay in the points near the limit cycle, which accounts for the delay between the stimulus and the oscillation.

2.5 Modelling of coupled systems

Neurons communicate through synapses: electrical connections between different parts of neurons, usually the dendrites from one neuron with the axon from another one. Synapses are very varied and can differ in many biological properties. One of the main ones is the excitatory or inhibitory character: excitatory synapses favor depolarization as they are triggered, whereas inhibitory counteract it. Mathematically, a synapse is modelled by adding an extra term to the potential equation. In our case we will use graded synapse, which means the strength of the synapse is variable. It contains the following elements:

- Maximal conductance: it is analogous to the gated channels conductance, so it accounts for the capability of electric current to flow through the connection.
- Activation function: it is similar to the gated channels: it takes a function between zero and one which represents how active the synapse is. Zero means the conductance is null, whereas one means the conductance reaches its maximal value. Just like the gating variables, it may have its own dynamics, meaning there is an extra equation ruling its value, or it can just be given by a function of another parameter, usually the voltage of the neuron that triggers the synapse.
- Potential difference: this term is similar to that of the gated channels. The sign and magnitude of the intensity depends on the potential difference with respect to a threshold value, V_0.

Combining all the terms, the expression for the synaptic current is:

$$I_{syn} = g \cdot s(V)(V - V_0)\,.$$

3. PRCs and PRFs

3.1 Phase and asymptotic phase

As previously mentioned, a cell in oscillatory state is represented by a system with a limit cycle. Since a limit cycle is a one dimensional curve in the phase space we can parameterize it by using one single variable: the **phase**. The phase is a periodic function and can have a explicit dependence on time, which we can remove by performing a change of variables.

In principle the phase is only defined on the limit cycle itself. However, there is a way of extending the concept of phase out of the cycle by using the concept of **asymptotic phase**.

Definition 3.1. Given a dynamical system $\dot{x} = X(x)$ with a stable limit cycle γ and flow $\phi_t(x)$, we say a point x in its basin of attraction has asymptotic phase θ if:

$$\lim_{t\to\infty} ||\phi_t(x) - \gamma(\theta(t))|| = 0\,. \tag{10}$$

This way we assign to each point in the attraction basin of the cycle a phase that corresponds to the point on the limit cycle towards which it tends asymptotically. Note that the asymptotic phase function is precisely the phase on the limit cycle:

$$\vartheta(\gamma(\theta)) = \theta\,.$$

However, when we are dealing with an excitable cell, the dynamical systems modelling it has a strong focus, so we have to extend the concept of phase even further. In this case we can define a phase by looking at equation expressed in polar coordinates under certain circumstances. Let us see the case where the focus is linear and expressed in normal form. Remember that the planar polar coordinates are defined by the following changes:

$$(r,\theta) = \rho(x,y), \quad \begin{cases} r = \rho_1(x,y) = \sqrt{x^2+y^2} \\ \theta = \rho_2(x,y) = \theta = \arctan\left(\frac{y}{x}\right) \end{cases}, \tag{11}$$

and therefore the linear strong focus writes in polar coordinates as:

$$\begin{pmatrix} \dot{x} \\ \dot{y} \end{pmatrix} = \begin{pmatrix} \alpha & -\beta \\ \beta & \alpha \end{pmatrix} \begin{pmatrix} x \\ y \end{pmatrix} \implies \begin{cases} \dot{r} = \frac{\partial r}{\partial x}\dot{x} + \frac{\partial r}{\partial y}r\dot{y} = \frac{x\dot{x}+\dot{y}y}{\sqrt{x^2+y^2}} = \frac{(\alpha x^2 - \beta yx + \alpha y^2 + \beta xy}{r} = \alpha r \\ \dot{\theta} = \frac{\partial \theta}{\partial x}\dot{x} + \frac{\partial \theta}{\partial y}\dot{y} = \frac{1}{1+\frac{y^2}{x^2}}\frac{\dot{y}x - y\dot{x}}{x^2} = \frac{\beta x^2 + \alpha yx - \alpha yx + \beta y^2}{r^2} = \beta \end{cases}. \tag{12}$$

Thus, θ **is independent of the radius**: trajectories spin around the center at constant angular speed. That is, radial lines are mapped by the flow into radial maps for every interval of time. In fact, we can compute the explicit flow:

$$\phi_t(r_0,\theta_0) = (r_0 e^{\alpha t}, \theta_0 + \beta t)\,. \tag{13}$$

This polar expression makes it intuitive to assign the same asymptotic phase to all the points lying on a segment from the origin, but we will see in the next section that the asymptotic phase can only be defined for foci under certain conditions.

3.2 Asymptotic phase for foci: isochrony conditions

We have seen in definition 3.1 that we are able to define a phase outside a limit cycle by means of the asymptotic phase . In that case, a point was assigned a certain asymptotic phase if it approached a point on the limit cycle at time infinity. However, on a focus this information would be trivial given that all points approach the equilibrium at infinite infinite. Instead, we will define the asymptotic phase by means of the **isochronous sections**:

Definition 3.2. Given a dynamical system with an equilibrium at x_0 with eigenvalues of the linearization having negative real part, basin of attraction $U \subset \mathbb{R}^n$ and whose flow we denote by $\phi_t(x)$; an **isochronous section** — or **isochron** — is a manifold $\Sigma \subset U$ such that there exists a real number $T \in \mathbb{R}$, $T > 0$ for which $\phi_T(x) \in \Sigma \ \forall x \in \Sigma$ but $\forall t < T \ \phi_T(x) \notin \Sigma$. Two points $x, y \in U$ are said to have **the same asymptotic phase** if they belong to the same isochronous section.

That is, an isochronous section is a manifold which has an associated period such that the flow for that period maps it to itself, and it allows us to define a phase around the focus. By definition, we can consider that each isochronous section defines a phase value, so we can write Σ_θ to denote the section determining the phase θ. In the case of linear foci — equation (**??**) — the polar expression makes it clear that

$$\Sigma_\theta = \{(r\cos(\theta), r\sin(\theta)), r \in \mathbb{R}\} \tag{14}$$

are isochronous sections, since in time 2π, and not before, the flow brings all those points to the same manifold. However, the existence of such sections is not trivial in nonlinear cases. In fact, in general, nothing ensures the existence of such sections since, for instance, angular speed could be dependent on radius. This motivates the following definition:

Definition 3.3. A dynamical system with an attracting focus is called an **isochronous system** if there exists one isochronous section.

We now discuss briefly some results that study the requirements a system needs to fulfill in order to be isochronous. From now on we will be dealing with planar systems, and it is worth recalling that, whenever a two times two matrix has a pair of conjugate eigenvalues $\lambda_1 = \alpha + i\beta$, $\lambda_2 = \alpha - i\beta$, it always admits the complex diagonal Jordan form, and the following real form:

$$\begin{pmatrix} \alpha & -\beta \\ \beta & \alpha \end{pmatrix}. \tag{15}$$

In this section we work with the diffeomorphism $\varphi : \mathbb{R}^2 \longrightarrow \mathbb{R}^2$, and we consider its differential acts on vector fields, so we use the pushforward notation. Note that the pushforward is defined on the tangent bundle of the original space, but in this case $T_x\mathbb{R}^2 \cong \mathbb{R}^2 \ \forall x \in \mathbb{R}^2$ and we can express it in coordinates. If φ is

$$\begin{array}{ccc} \varphi : U \subset \mathbb{R}^2 & \longrightarrow & U' \subset \mathbb{R}^2 \\ (u, v) & \mapsto & (\varphi_1(u, v), \varphi_2(u, v)) \end{array},$$

then $\varphi_* : \mathbb{R}^2 \longrightarrow \mathbb{R}^2$ and

$$\varphi_*(v_1, v_2) = \begin{pmatrix} \frac{\partial \varphi_1}{\partial u} & \frac{\partial \varphi_1}{\partial v} \\ \frac{\partial \varphi_2}{\partial u} & \frac{\partial \varphi_2}{\partial v} \end{pmatrix} \begin{pmatrix} v_1 \\ v_2 \end{pmatrix}.$$

In the following theorem ρ denotes the change from Cartesian to polar coordinates.

Theorem 3.4 (J. Giné and M. Grau,[10]). *For an analytic system whose linear part is a strong focus, that is*

$$\begin{pmatrix} \dot{x} \\ \dot{y} \end{pmatrix} = \begin{pmatrix} \alpha & -\beta \\ \beta & \alpha \end{pmatrix} \begin{pmatrix} x \\ y \end{pmatrix} + \begin{pmatrix} f_1(x,y) \\ f_2(x,y) \end{pmatrix},$$

with $\frac{\partial}{\partial x_i} f_1\Big|_{t=0}(0,0) = \frac{\partial}{\partial x_i} f_2\Big|_{t=0}(0,0) = 0$, *the following statements are equivalent:*

1. *There exist a neighborhood of the origin U and an analytic change of variables $\varphi : U \to U$ such that φ is locally the identity, $\varphi_*(0,0) = I$, and such that the angular speed expressed in polar coordinates is independent of the radius:*

$$\rho_* \varphi_*(X) = \begin{pmatrix} rf(r,\theta) \\ g(\theta) \end{pmatrix}.$$

2. *There exists an analytic vector field Y, which has a star node; that is, to order one near the origin it is radial:*

$$Y = \begin{pmatrix} x + o(2) \\ y + o(2) \end{pmatrix},$$

such that it is **a normalizer of** X, *that is*

$$[X, Y] = \mu(x,y)Y, \text{ with } \mu(x,y) \in \mathbb{R} \text{ and } \mu(0,0) = 0\,. \tag{16}$$

3. *There exists a section Σ such that the period function $\tau : \Sigma \to \mathbb{R}^+$ is constant.*

This theorem implies that we have several ways of evaluating the isochronicity: on the one hand, we can look for a change of variables that turns the system into one that whose angular speed does not depend on the radius; on the other hand, we can look for a normalizer with a star node. In the next sections we exploit both properties, first looking for the change of variables and using it to compute the field Y, following some ideas in [12]. The relevance of the field Y comes from its direct relation with the isochronous sections.

Theorem 3.5 (Algaba and Reyes,[2]). *The origin is an isochronous point if and only if there exists a smooth vector field $Y = \begin{pmatrix} x + o(2) \\ y + o(2) \end{pmatrix}$, such that $[X, Y] = \mu(x,y)Y$, where $\mu(x,y)$ is a smooth function such that $\mu(0,0) = 0$. Besides, the orbits of Y in a neighborhood of the origin are isochronous sections.*

We should point out that **the field Y is not unique**. However, two different fields satisfying the condition are proportional to one another (see [2]), so they produce the same flow lines, and therefore the same isochronous sections.

Another important remark is the fact that, whenever a system is isochronous, the asymptotic phase in a neighborhood of the equilibrium is well defined, as there is one single isochrons passing through every point:

Theorem 3.6 (Algaba and Reyes, [2]). *The origin is an isochronous point of the system if and only if it has an infinite number of isochronous sections. Besides, if it is a focus, then the isochronous are disjoint and there is a unique isochronous arriving at the center with a given direction.*

Note that in the particular case of the linear focus, this infinite set of isochrons is given by the radial vectors from the equilibrium.

Theorems 3.4 and 3.5 tell us that if there is a local change of coordinates that linearizes the system (in that case the angular speed is constant, see (**??**)) then the centre is isochronous, there exists a normalizer field Y such that $[X, Y] = \mu Y$ and the isochronous sections correspond to the orbits of Y. Besides, the normal form theorem by Poincaré tells us that a strong focus is always linearizable, so this condition will be fulfilled in the case of an excitable neuron. We now provide a constructive proof of Poincaré's theorem for this case writing out all the details that are relevant for our numerical implementation.

Theorem 3.7 (Poincaré)**.** *For a planar dynamical system*

$$\begin{pmatrix} \dot{x} \\ \dot{y} \end{pmatrix} = X(x, y) = \begin{pmatrix} X_1(x, y) \\ X_2(x, y) \end{pmatrix}, \tag{17}$$

with an equilibrium at $(\tilde{x}, \tilde{y})$ *a pair of complex conjugate eigenvalues* $\lambda_{1,2} = \alpha \pm i\beta$, $\alpha \cdot \beta \neq 0$ *— a strong focus — there exists a local change of coordinates — a diffeomorphism — in a neighborhood of* $(\tilde{x}, \tilde{y})$

$$\varphi(u, v) = \begin{pmatrix} x(u, v) \\ y(u, v) \end{pmatrix},$$

such that the dynamics in (u, v) *is linear:*

$$\begin{pmatrix} \dot{u} \\ \dot{v} \end{pmatrix} = \begin{pmatrix} \alpha & -\beta \\ \beta & \alpha \end{pmatrix} \begin{pmatrix} u \\ v \end{pmatrix}. \tag{18}$$

Proof. We perform the change of variable in three stages; the final change of variable will be the composition of all of them.

1. First **we offset the system to place the equilibrium at the origin**. This means we apply the following change of variables:

$$(x_1, y_1) = T(x, y) = (x - \tilde{x}, y - \tilde{y}) \implies \begin{pmatrix} \dot{x}_1 \\ \dot{y}_1 \end{pmatrix} = \tilde{X}(x_1, y_1). \tag{19}$$

2. Then, **we perform a linear change of coordinates** to transform the linear part of the system into canonical Jordan form. Let the linear part of the system be

$$D\tilde{X}(0, 0) = \begin{pmatrix} a & b \\ c & d \end{pmatrix}. \tag{20}$$

   Given that the eigenvalues of this matrix are complex conjugates the focus condition holds:

$$\sqrt{4(ad - bc) - (a + b)^2} < 0.$$

   We write the nonlinear part of the system in the following way:

$$\tilde{X}(x_1, y_1) = \begin{pmatrix} a & b \\ c & d \end{pmatrix} \begin{pmatrix} x_1 \\ y_1 \end{pmatrix} + \begin{pmatrix} f_1(x_1, y_1) \\ f_2(x_1, y_1) \end{pmatrix}. \tag{21}$$

where $\left.\frac{\partial f_j}{x_i}\right|_{(\tilde{x},\tilde{y})} = 0$ for $i, j \in (1, 2)$. We denote the real and imaginary part of the eigenvalues by α and β, respectively:

$$\begin{cases} \lambda_1 = \frac{a+d}{2} + \frac{i}{2}\sqrt{-(a+d)^2 + 4(ad-bc)} = \alpha + i\beta \\ \lambda_2 = \frac{a+d}{2} - \frac{i}{2}\sqrt{-(a+d)^2 + 4(ad-bc)} = \alpha - i\beta \end{cases} . \tag{22}$$

The corresponding eigenvectors are:

$$\left\{ v_1 = \begin{pmatrix} b \\ -a + (\alpha + i\beta) \end{pmatrix}, v_2 = \begin{pmatrix} b \\ -a + (\alpha - i\beta) \end{pmatrix} \right\} . \tag{23}$$

This pair of complex vectors brings the matrix into the complex diagonal form:

$$Q^{-1} D\tilde{X}(0,0) Q = \begin{pmatrix} \lambda_1 & 0 \\ 0 & \lambda_2 \end{pmatrix} . \tag{24}$$

And by taking the real and complex parts of the eigenvectors,
$\{\Re(v_1), \Im(v_1)\} = \left\{ \begin{pmatrix} b \\ \alpha - a \end{pmatrix}, \begin{pmatrix} 0 \\ -\beta \end{pmatrix} \right\}$, we can transform it into the real canonical form:

$$\begin{aligned} P &= \begin{pmatrix} b & 0 \\ \alpha - a & -\beta \end{pmatrix}, \\ P^{-1} A P &= \begin{pmatrix} \alpha & -\beta \\ \beta & \alpha \end{pmatrix} . \end{aligned} \tag{25}$$

Thus, the second change of variables is:

$$\begin{pmatrix} x_2 \\ y_2 \end{pmatrix} = P^{-1} \begin{pmatrix} x_1 \\ y_1 \end{pmatrix} . \tag{26}$$

When we apply this change to the dynamical system we have:

$$\begin{aligned} \begin{pmatrix} \dot{x_1} \\ \dot{y_1} \end{pmatrix} &= P \begin{pmatrix} \dot{x_2} \\ \dot{y_2} \end{pmatrix} = AP \begin{pmatrix} x_2 \\ y_2 \end{pmatrix} + \begin{pmatrix} f_1(P(x_2, y_2)^T) \\ f_2(P(x_2, y_2)^T) \end{pmatrix}, \\ \begin{pmatrix} \dot{x_2} \\ \dot{y_2} \end{pmatrix} &= \underbrace{P^{-1} A P}_{\text{Jordan real form}} \begin{pmatrix} x_2 \\ y_2 \end{pmatrix} + P^{-1} \begin{pmatrix} \tilde{f}(x_2, y_2) \\ \tilde{f}(x_2, y_2) \end{pmatrix} . \end{aligned} \tag{27}$$

We can remove the indices and have so far the following system:

$$\begin{pmatrix} \dot{x} \\ \dot{y} \end{pmatrix} = \underbrace{\begin{pmatrix} \alpha & -\beta \\ \beta & \alpha \end{pmatrix}}_{\tilde{A}} \begin{pmatrix} x \\ y \end{pmatrix} + \begin{pmatrix} g_1(x, y) \\ g_2(x, y) \end{pmatrix} . \tag{28}$$

3. Once the linear part has canonical form we can apply **normal form transformations**. Let us assume the first order of the g functions is n, so we can write $\mathbf{g} = \mathbf{g_n} + o(n+1)$ We use the *ansatz*

$(x,y) = (u(x,y), v(x,y)) = (u + h_x(u,v), v + h_y(u,v))$, where $h_x(x,y)$ and $h_y(x,y)$ are homogeneous polynomials of degree n in the variables x, y. This gives us:

$$\left[\begin{pmatrix} 1 & 0 \\ 0 & 1 \end{pmatrix} + \begin{pmatrix} \partial_x h_x & \partial_y h_x \\ \partial_x h_y & \partial_y h_y \end{pmatrix}\right] \begin{pmatrix} \dot{u} \\ \dot{v} \end{pmatrix} = \begin{pmatrix} \alpha & -\beta \\ \beta & \alpha \end{pmatrix} \begin{pmatrix} u + h_x \\ v + h_y \end{pmatrix} + \\ + \begin{pmatrix} g_1(u + h_x(u,v), v + h_x(u,v)) \\ g_2(u + h_x(u,v), v + h_y(u,v)) \end{pmatrix},$$

$$\begin{pmatrix} \dot{u} \\ \dot{v} \end{pmatrix} = \underbrace{\left[\begin{pmatrix} 1 & 0 \\ 0 & 1 \end{pmatrix} + \begin{pmatrix} \partial_x h_x & \partial_y h_x \\ \partial_x h_y & \partial_y h_y \end{pmatrix}\right]^{-1}}_{(I+D\mathbf{h})^{-1}} \left[\begin{pmatrix} \alpha & -\beta \\ \beta & \alpha \end{pmatrix} \begin{pmatrix} u + h_x \\ v + h_y \end{pmatrix} + \begin{pmatrix} \tilde{g}_1(u,v) \\ \tilde{\mathbf{g}}_2(u,v) \end{pmatrix}\right]$$

$$\dot{\mathbf{u}} = \tilde{A}\mathbf{u} + \underbrace{(\tilde{A}\mathbf{h} - D\mathbf{h}\tilde{A}\mathbf{u}) + \mathbf{g_n}}_{(*)} + o(n+1)\,. \tag{29}$$

We can eliminate the terms of degree n by equating $(*)$ to zero and solving for h_x and h_y. If we consider the planar vector fields $\tilde{A}x = \begin{pmatrix} \alpha & -\beta \\ \beta & \alpha \end{pmatrix} \begin{pmatrix} x \\ y \end{pmatrix} = \begin{pmatrix} \alpha x - \beta y \\ \beta x + \alpha y \end{pmatrix}$ and $h = \begin{pmatrix} h_x(u,v) \\ h_y(u,v) \end{pmatrix}$, $(*)$ can be rewritten as:

$$(\tilde{A}\mathbf{h} - D\mathbf{h}\tilde{A}\mathbf{u}) + \tilde{\mathbf{g}}_n = 0,$$
$$[\tilde{A}\mathbf{u}, \mathbf{h}] = -\tilde{\mathbf{g}}_n\,. \tag{30}$$

where $[\tilde{A}\mathbf{x}, \mathbf{h}]$ is the Lie bracket of the vector fields. As usually in normal form calculations, we write this expression as a linear operator generated by $\tilde{A}$ on the space of homogeneous polynomial vector fields, $[\tilde{A}\mathbf{u}, \mathbf{h}] = L_{\tilde{A}}(\mathbf{h})$. In order to show that the system can be linearized, we only need to show that this linear operator is invertible. Therefore, the removable terms of $\mathbf{g}$ are those that can be produced by inserting the right h into the operator L_A. In other words, $\mathrm{Im}(L_A)$ is what determines what we can remove and what not. Let us see that in the case of strong foci this operator spans the whole space of homogeneous polynomials H^n, so all we can remove all terms. From now on we can drop the tilde from $\tilde{A}$. In a strong focus we have:

$$A = \begin{pmatrix} \alpha & -\beta \\ \beta & \alpha \end{pmatrix}.$$

We can study $\mathrm{Im}(L_A)$ by looking at its matrix form using the basis $\mathcal{B}(H^n) = \{e^a, e_a\}$, $a \in (0, \dots, n)$, where $e^a = \begin{pmatrix} u^{n-a}v^a \\ 0 \end{pmatrix}$ and $e_a = \begin{pmatrix} 0 \\ u^{n-a}v^a \end{pmatrix}$.

$$L_A(e^a) = \begin{pmatrix} \alpha & -\beta \\ \beta & \alpha \end{pmatrix} \begin{pmatrix} u^{n-a}v^a \\ 0 \end{pmatrix} - \begin{pmatrix} (n-a)u^{n-a-1}v^a & au^{n-a}v^{a-1} \\ 0 & 0 \end{pmatrix} \begin{pmatrix} \alpha u - \beta v \\ \beta u + \alpha v \end{pmatrix} = \\ = \begin{pmatrix} \alpha(1-n)u^{n-a}v^a + \beta(n-a)u^{n-a-1}v^{a+1} - \beta a u^{n-a+1}v^{a-1} \\ \beta u^{n-a}v^a \end{pmatrix}.$$

$$Ł_A(e_a) = \begin{pmatrix} \alpha & -\beta \\ \beta & \alpha \end{pmatrix} \begin{pmatrix} 0 \\ u^{n-a}v^a \end{pmatrix} - \begin{pmatrix} 0 & 0 \\ (n-a)u^{n-a-1}v^a & au^{n-a}v^{a-1} \end{pmatrix} \begin{pmatrix} \alpha u - \beta v \\ \beta u + \alpha v \end{pmatrix} = \\ = \begin{pmatrix} -\beta u^{n-a}v^a \\ \alpha(1-n)u^{n-a}v^a + \beta(n-a)u^{n-a-1}v^{a+1} - \beta a u^{n-a+1}v^{a-1} \end{pmatrix}.$$

That is,

$$\begin{cases} L_A(e^a) = \alpha(1-n)e^a + \beta(n-a)e^{a+1} - \beta a e^{a-1} + \beta e_a \\ L_A(e_a) = \alpha(1-n)e_a + \beta(n-a)e_{a+1} - \beta a e_{a-1} - \beta e^a \end{cases} . \tag{31}$$

This means that, for two-variable homogeneous polynomials of degree n, the operator has the following form:

$$L_A = \left(\begin{array}{cccc:cccc} \alpha(1-n) & \dots & 0 & 0 & -\beta & \dots & 0 & 0 \\ n\beta & \dots & 0 & 0 & 0 & \dots & 0 & 0 \\ \vdots & \ddots & \vdots & \vdots & \vdots & \ddots & \vdots & \vdots \\ 0 & \dots & -(n-1)\beta & 0 & 0 & \dots & 0 & 0 \\ 0 & \dots & \alpha(1-n) & -n\beta & 0 & \dots & -\beta & 0 \\ 0 & \dots & \beta & \alpha(1-n) & 0 & \dots & 0 & -\beta \\ \hdashline \beta & 0 & 0 & 0 & \alpha(1-n) & \dots & 0 & 0 \\ 0 & \dots & 0 & 0 & 0 & \dots & 0 & 0 \\ \vdots & \ddots & \vdots & \vdots & \vdots & \ddots & \vdots & \vdots \\ 0 & \dots & 0 & 0 & 0 & \dots & -(n-1)\beta & 0 \\ 0 & \dots & \beta & 0 & 0 & \dots & \alpha(1-n) & -n\beta \\ 0 & \dots & 0 & \beta & 0 & \dots & \beta & \alpha(1-n) \end{array}\right) . \tag{32}$$

Let us examine the conditions for the operator L_A of a diagonal matrix A to have a non-null kernel in the space of homogeneous polynomials of degree n. Considering the matrix A as an endomorphism of $\mathbb{C}^2$, its normal Jordan form is diagonal:

$$A = \begin{pmatrix} \lambda_1 & 0 \\ 0 & \lambda_2 \end{pmatrix} .$$

Computing L_A for this diagonal form on the elements of the basis:

$$\begin{aligned} L_A(e^a) &= \begin{pmatrix} \lambda_1 & 0 \\ 0 & \lambda_2 \end{pmatrix} \begin{pmatrix} u^{n-a}v^a \\ 0 \end{pmatrix} - \begin{pmatrix} (n-a)u^{n-a-1}v^i & au^{n-a}v^{a-1} \\ 0 & 0 \end{pmatrix} \begin{pmatrix} \lambda_1 u \\ \lambda_2 v \end{pmatrix} = \\ &= \begin{pmatrix} \lambda_1 u^{n-a}v^a \\ 0 \end{pmatrix} - \begin{pmatrix} \lambda_1(n-a)u^{n-a}v^a + \lambda_2 a u^{n-a}v^a \\ 0 \end{pmatrix} = \begin{pmatrix} (\lambda_1 - ((n-a)\lambda_1 + a\lambda_2))u^{n-a}v^a \\ 0 \end{pmatrix} . \\ L_A(e_a) &= \begin{pmatrix} \lambda_1 & 0 \\ 0 & \lambda_2 \end{pmatrix} \begin{pmatrix} 0 \\ u^{n-a}v^a \end{pmatrix} - \begin{pmatrix} 0 & 0 \\ (n-a)u^{n-a-1}v^a & au^{n-a}v^{a-1} \end{pmatrix} \begin{pmatrix} \lambda_1 u \\ \lambda_2 v \end{pmatrix} = \\ &= \begin{pmatrix} 0 \\ \lambda_2 u^{n-a}v^a \end{pmatrix} - \begin{pmatrix} 0 \\ \lambda_1(n-a)u^{n-a}v^a + \lambda_2 a u^{n-a}v^a \end{pmatrix} = \begin{pmatrix} 0 \\ (\lambda_2 - ((n-a)\lambda_1 + a\lambda_2))u^{n-a}v^a \end{pmatrix} . \end{aligned}$$

That is,

$$\begin{cases} L_A(e^a) = [\lambda_1 - (n-a)\lambda_1 - a\lambda_2]e^a \\ L_A(e_a) = [\lambda_2 - (n-a)\lambda_1 - a\lambda_2]e_a \end{cases} . \tag{33}$$

Therefore, we see the $2(n+1)$ vectors of the basis are eigenvectors, which means L_A, considered as an operator on the space of homogeneous polynomials of degree n, diagonalizes. Thus, if the kernel

were non-null some of the eigenvalues would be zero. In our case the complex eigenvalues of A are $\lambda_1 = \alpha + i\beta$ and $\lambda_2 = \alpha - i\beta$. Solving for zero the equation for $L_A(e^a)$ we have:

$$\begin{aligned} &(\alpha + i\beta) - (n-a)(\alpha + i\beta) - a(\alpha - i\beta) = 0 \\ &\alpha - (n-a)\alpha - a\alpha = 0 \implies n - 1 = 0 \implies n = 1\,. \end{aligned} \tag{34}$$

Likewise, for the second one,

$$\begin{aligned} &(\alpha - i\beta) - (n-a)(\alpha + i\beta) - a(\alpha - i\beta) = 0 \\ &\alpha - (n-a)\alpha - a\alpha = 0 \implies n - 1 = 0 \implies n = 1\,. \end{aligned} \tag{35}$$

Therefore, there are no zero eigenvalues for $n > 1$, which is precisely the case we are interested in, since L_A acts on nonlinear polynomials. Note that if $\alpha = 0$ this restriction disappears and resonant monomials appear. If there are no resonant terms in the complex case there cannot be resonant terms in the non complex one.

Since our L_A operator has null kernel for all the nonlinear terms $\mathbf{g_n}$ there exists an $\mathbf{h}$ that solves (30). In order to solve it we only need to express $\mathbf{g}_n$ in the basis $\mathcal{B}$ and solve the linear equation

$$L_A \mathbf{h_n} = -\mathbf{g}_n \implies \mathbf{h_n} = -L_A^{-1}\mathbf{g}_n\,. \tag{36}$$

This way we obtain the n-degree homogeneous polynomial $\mathbf{h}_n$ expressed in the basis $\mathcal{B}$. By replacing $\mathbf{h}_n$ in (29) we obtain a new expression for the system without terms of order n. Proceeding recursively we can eliminate terms up to any order. Note that, whenever we calculate $\mathbf{h}$ and perform the change of variables, the higher order terms are modified and have to be updated in order to perform the next step. Once we have removed terms of order up to n we obtain our complete expression for the change of variables:

$$\begin{cases} \mathbf{x} = \mathbf{x}_0 + \mathbf{x}_{eq} := \varphi_{\text{center}}(\mathbf{x}_0) \\ \mathbf{x}_0 = P^{-1}\mathbf{x}_{Jordan} := \varphi_{Jordan}(\mathbf{x}_0) \\ \mathbf{x}_{Jordan} = \mathbf{u}_1 + \mathbf{h}_1(\mathbf{u}_1) := \varphi_1(\mathbf{u}_1) \\ \mathbf{u}_1 = \mathbf{u}_2 + \mathbf{h}_2(\mathbf{u}_2) := \varphi_2(\mathbf{u}_2) \\ \vdots \\ \mathbf{u}_{n-1} = \mathbf{u}_n + \mathbf{h}_n(\mathbf{u}_n) := \varphi_n(\mathbf{u}_n) \end{cases} \tag{37}$$

The system is linear up to order n in the coordinates $\mathbf{u}_n$. Therefore,

$$\mathbf{x} = \varphi_{\text{center}} \circ \varphi_{\text{Jordan}} \circ \varphi_1 \circ \cdots \circ \varphi_n(\mathbf{u}_n) := \varphi(\mathbf{u}_n)\,, \tag{38}$$

with inverse change

$$\mathbf{u}_n = \varphi_n^{-1} \circ \cdots \circ \varphi_1^{-1} \circ \varphi_{\text{Jordan}}^{-1} \circ \varphi_{\text{center}}^{-1}(\mathbf{x}) := \varphi^{-1}(\mathbf{x})\,. \tag{39}$$

□

To summarize, whenever we have a strong focus, which is the case for an excitable cell, it is possible to linearize the system and, as a consequence it is isochronous and it makes sense to talk about asymptotic phase.

3.3 Phase resetting curves

As we have mentioned previously, when we have a limit cycle in our system we can parameterize it by one variable, the phase, in order to obtained a simplified description. The classical study of perturbations of oscillations consists in analyzing the change of phase in an oscillatory system when a stimulus is applied at a certain point along the oscillation. This means that, at a given θ, a stimulus $\vec{\epsilon}$ is applied to the system dragging it off the limit cycle. However, since this cycle is stable and the perturbation is small, it quickly returns to the oscillation at a different point, that is, with a different phase. The same perturbation has a different effect on the cycle depending on the point of the cycle where we apply it.

Definition 3.8. The relation between a point on a limit cycle described by a phase θ and the new phase it is displaced to when a stimulus is applied is referred to as **phase shifting**. The difference between the shifted phase and the original phase as a function of the point of the limit cycle where we apply the perturbation is known as **phase resetting**, and we denote it by:

$$\Delta\theta = \theta' - \theta\,. \tag{40}$$

The fact that the phase resetting varies according to the point of the cycle where the stimulus is applied motivates the following definition:

Definition 3.9. Given a limit cycle parameterized by a phase θ, the **Phase Resetting Curve** (PRC) for a certain stimulus is the function that assigns to each value of θ its corresponding phase resetting value. We this function also by $\mathrm{PRC}(\theta) = \theta' - \theta$. Similarly, the function that maps every phase θ to the new phase θ' is referred to as **Phase Transition Curve** (PTC).

Phase resetting curves are an interesting theoretical tool to describe the effect of perturbations on systems, but they are also experimentally measured by actually producing stimuli and observing the variations in the period that follows. In biological oscillatory systems two types of PTCs have been observed:

- **Type 0, or strong type**: the PTC is not invertible. This means a stimulus applied at different phases resets the phase to the same value. This would be the case if, for instance, a stimulus was intense enough to bring a neuron to spiking regardless of when it is applied. In that case, the PTC would be constant with value 0, considering the spiking occurs at $\theta = 0$.
- **Type 1, or strong type**: the PTC is an invertible map. This means the stimulus has a different effect for each phase value where it is applied.

The classical approach — see in [8] — to phase resetting curve computation is the use of the so-called **adjoint method**. This method gives the phase resetting curve for the points on a limit cycle,γ. If we consider the asymptotic phase ϑ as a function of space, we can obtain a first order approximation of the effect of an stimulus $\vec{\epsilon}$ applied to a point in the limit cycle $\gamma(\theta)$ by using its gradient:

$$\vartheta(\gamma(\theta) + \vec{\epsilon}) \approx \vartheta(\gamma(\theta)) + \nabla\vartheta_{\gamma(\theta)}(\vec{\epsilon}) = \theta + \nabla\vartheta_{\gamma(\theta)} \cdot \vec{\epsilon}\,. \tag{41}$$

This means we can have a linear approximation of the phase resetting curve if we compute the gradient of ϑ on the limit cycle $\gamma(\theta)$:

$$\mathrm{PRC}(\theta) = \vartheta(\gamma(\theta) + \vec{\epsilon}) - \theta = \nabla\vartheta_{\gamma(\theta)} \cdot \vec{\epsilon}\,. \tag{42}$$

The adjoint method bases on computing this gradient as the solution of the following differential equation with a periodicity condition — see [8]:

$$\begin{cases} \frac{d\nabla\vartheta_{\gamma(\theta)}}{dt} = -DX^T(\gamma(\theta)) \\ \nabla\vartheta_{\gamma(\theta)}(T) = \nabla\vartheta_{\gamma(\theta)}(0) \end{cases} . \tag{43}$$

Therefore, **we can compute the phase resetting curve on a limit cycle by solving the adjoint equation** to obtain the asymptotic phase gradient and by multiplying by the infinitesimal stimulus. We emphasize that this adjoint equation is only valid for the points located on the limit cycle.

Other studies have extended this approach to perturbations applied to points that are not on the limit cycle, with the aim of analyzing sequential perturbations where the time between them is very short or other types of perturbations that do not allow the system to return to the oscillatory state. In [12] the authors show how to use the parameterization method — see [9] — to parameterize the dynamics of the system in a neighborhood of a stable limit cycle. They find a parameterization $K(\theta, \sigma)$ for that neighborhood in such a way that the dynamics expressed in the coordinates θ and σ correspond to the phase advancement and a movement in a direction transversal to the limit cycle. This results in a natural expression of the asymptotic phase, namely the variable θ itself. By finding an appropriate vector field Y transversal to the limit cycle they show that the asymptotic phase gradient has an explicit expression

$$\nabla\vartheta(\sigma, \theta) = \frac{Y^\perp(\sigma, \theta)}{T(Y^\perp(\sigma, \theta) \cdot X)} , \tag{44}$$

where T is the period of the cycle. This allows to extend the phase resetting curves outside, so we can refer to them as **Phase Resetting Functions** (PRF). While phase resetting curves give a description of the changes in the phase of a limit cycle produced by a stimulus, phase resetting functions describe the effect of stimuli on the asymptotic phase for the region where it is defined. Note that, since the asymptotic phase on a limit cycle coincides with its phase, the phase resetting function on a limit cycle coincides with the phase resetting curves.

3.4 Theoretical result for the computation of $\nabla\vartheta$

As we have seen in section 3.2, a system with a strong focus is linearizable around the equilibrium by a diffeomorphism φ. In this section we consider this kind of system, and denote by (u, v) the variables where the dynamics are linear, and (x, y) the original variables of the system. As in equation (38), $(x, y) = \varphi(u, v)$. The tildes denotes functions or values in the linearized system and linear variables (u, v).

Theorems 3.4 and 3.5 state that the isochronicity condition is equivalent to the existence of a field Y whose orbits are the isochrons. On the other hand, theorem 3.7 ensures a system with a strong focus is isochronous. Combining these facts, we deduce that for a system with a strong focus the existence of this Y is ensured. Let us recall the properties of Y: it is a normalizer of X, it has a star node at the origin and its flow lines are ischrons. We are going to see that computing Y is a key point to obtaining $\nabla\vartheta$.

The gradient of the asymptotic phase is perpendicular to the isochrons; but let us analyze the nonlinear case and the perpendicularity relation to the field Y. Given a point in the nonlinear variables (x, y), its asymptotic phase is defined in terms of the corresponding linear phase, that is:

$$\vartheta(x, y) = \tilde{\vartheta} \circ \varphi^{-1}(x, y) = \tilde{\vartheta}(u, v) , \tag{45}$$

where $\tilde{\vartheta}$ is the phase function in the linear space, defined by the radial isochrons, see (14). Theorem 3.5 tells us that the normalizer field has the isochrons as integral curves. Since this field is important for computing $\nabla\vartheta$ we are going to show some of its properties. The radial sections are the orbits of the radial field

$$\tilde{Y} = \frac{\partial}{\partial u} + \frac{\partial}{\partial v}\,, \tag{46}$$

which, indeed, satisfies the normalization relation of theorem 3.4:

$$\begin{aligned}[X, Y] &= [(\alpha u - \beta v)\partial_u + (\alpha v + \beta u)\partial_v), u\partial_u + v\partial_v] = \\ &= \left(\begin{pmatrix} \alpha & -\beta \\ \beta & \alpha \end{pmatrix}\begin{pmatrix} u \\ v \end{pmatrix} - \begin{pmatrix} 1 & 0 \\ 0 & 1 \end{pmatrix}\begin{pmatrix} \alpha u - \beta v \\ \alpha v + \beta u \end{pmatrix}\right) = \\ &= \begin{pmatrix} \alpha u - \beta v \\ \beta u + \alpha v \end{pmatrix} - \begin{pmatrix} \alpha u - \beta v \\ \alpha v + \beta v \end{pmatrix} = \begin{pmatrix} 0 \\ 0 \end{pmatrix}\end{aligned} \tag{47}$$

with $\mu = 0$. Let us show that the pushforward of this field by φ is the field with the star node of theorem 3.4 in the nonlinear variables. If we consider the gradient of the asymptotic phase,

$$\nabla\tilde{\vartheta} = \left(\frac{\partial\vartheta}{\partial u}, \frac{\partial\vartheta}{\partial v}\right)\,, \tag{48}$$

it has to be perpendicular to the level curves of the phase — the isochrons —, so it has to be perpendicular to $\tilde{Y}$:

$$\langle\nabla\tilde{\vartheta}, \tilde{Y}\rangle_{u,v} = 0\,.$$

In the nonlinear variables, we take $Y(x, y) := \varphi_* Y(\tilde{u}, v)$ and the gradient, following (45) using the chain rule:

$$\nabla\vartheta(x, y) = \nabla(\tilde{\vartheta}\circ\varphi^{-1}(x, y)) = \nabla\tilde{\vartheta}(\varphi^{-1}(x, y))\cdot\varphi_*^{-1}(x, y) = \nabla\tilde{\vartheta}(u, v)\cdot\varphi_*^{-1}(x, y)\,. \tag{49}$$

Therefore:

$$\langle\nabla\vartheta, Y\rangle_{(x,y)} = \nabla\tilde{\vartheta}(u, v)\cdot\varphi_{*(x,y)}\cdot\varphi^{-1}_{*(x,y)}\cdot\tilde{Y}(u, v) = \langle\tilde{Y}, \nabla\tilde{\vartheta}\rangle_{(u,v)} = 0\,, \tag{50}$$

which means Y is perpendicular to the gradient of the phase:

$$\nabla\vartheta = CY^T\,, \tag{51}$$

where $C \in \mathbb{R}$ is a normalization constant. In order to obtain this constant, we can follow the remark in [12]. Recall the linear dynamics is $\tilde{X} = \alpha r\frac{\partial}{\partial r} + \beta\frac{\partial}{\partial\theta}$, so considering the flow $\tilde{\phi}_t$ of a point (u, v) in the linear variables,

$$\begin{cases} \frac{d}{dt}\tilde{\vartheta}(\tilde{\phi}_t) = \beta \\ \frac{d}{dt}\tilde{\vartheta}(\phi_t) = \nabla\tilde{\vartheta}\cdot\frac{d}{dt}\tilde{\phi}(t) = \nabla\tilde{\vartheta}\cdot\tilde{X}(\tilde{\phi}(t)) \end{cases} \implies \langle\nabla\vartheta, \tilde{X}\rangle = C\langle\tilde{Y}^T, \tilde{X}\rangle = \beta\,. \tag{52}$$

This scalar product is the same for the nonlinear coordinates:

$$\langle\nabla\vartheta, X\rangle_{(x,y)} = \nabla\tilde{\vartheta}(u, v)\cdot\varphi^{-1}_{*(x,y)}\cdot\varphi_{*(x,y)}\cdot\tilde{X}(u, v) = \langle\nabla\tilde{\vartheta}, \tilde{X}\rangle_{(u,v)} = 0\,, \tag{53}$$

so we obtain a formula for the asymptotic phase:

$$\nabla\vartheta = \beta\frac{Y^T}{\langle X, Y^T\rangle}\,. \tag{54}$$

Since Y is defined as the pushforward of the field $\tilde{Y}(u,v)$, in order to be able to compute its commutators and show the normalization property we use the following lemma:

Lemma 3.10. *Given two neighborhoods $U \subset \mathbb{R}^n$ and $V \subset \mathbb{R}^n$, two vector fields $X, Y \in \mathfrak{X}(U)$ and a smooth map $\varphi : U \to V$ then the Lie bracket operator commutes with the pushforward of the map:*

$$\varphi_*[X, Y] = [\varphi_*(X), \varphi_*(Y)]\,. \tag{55}$$

Proof. This result is actually almost a consequence of the definition of the pushforward of a vector field. If we define a field at each point as an equivalence class of curves, then the pushforward is the derivative of the curve transformed under the function φ. Thus,

$$\begin{cases}\gamma(0) = u\\ \frac{d}{dt}\gamma(t)\big|_{t=0} = X\end{cases} \implies \begin{cases}\varphi\circ\gamma(0) = \varphi(u) = x\\ \frac{d}{dt}\varphi\circ\gamma(t)\big|_{t=0} = \varphi_*(X)\end{cases}\,. \tag{56}$$

This means if $\gamma(t)$ is an integral curve of X at u, so $\varphi\circ\gamma(t)$ is an integral curve of $\varphi_*(X)$ at $\varphi(u) = x$. On the other hand, when we apply a vector field to a function, the result is the derivative of the composition of the function with the integral curve of the vector field at that point. Since $\varphi\circ\gamma(t)$ is the integral curve of $\varphi_*(X)$, we have:

$$\varphi_*(X)(f)(\varphi(u)) = \frac{d}{dt}\, f\circ\varphi\circ\gamma(t)|_{t=0} = X(f\circ\varphi)(u)\,. \tag{57}$$

This last equation is just the result of *reorganizing function composition*. If we apply equation (57) to the vector field $[X, Y]$ we obtain:

$$\begin{aligned}\varphi_*[X, Y](f)(\varphi(u)) &= [X, Y](f\circ\varphi) = X(Y(f\circ\varphi)(u)) - Y(X(f\circ\varphi)(u)) =\\ &= X(\varphi_*(Y)(f)(\varphi(u))) - Y(\varphi_*(X)(f)(\varphi(u))) =\\ &= X(\varphi_*(Y))(f(\varphi(u)) - Y(\varphi_*(X))(f(\varphi(u)) =\\ &= \varphi_*(X)\varphi_*(Y)(f(u)) - \varphi_*(Y)\varphi_*(X)(f(u)) =\\ &= [\varphi_*(X), \varphi_*(Y)](f(u))\,.\end{aligned} \tag{58}$$

This proves the result. □

We can now show the normalization condition

Proposition 3.11. *The radial field given by $Y(x,y) = Y(\varphi(u,v)) = \varphi_*(u,v)\begin{pmatrix}u\\ v\end{pmatrix}$ is a normalizer of the vector field X .*

Proof. At a point $(x,y) = \varphi(u,v)$, we have:

$$\begin{cases}X(x,y) = \varphi_*\left[(\alpha u - \beta v)\partial_u + (\alpha v + \beta u)\partial_v\right]\\ Y(x,y) = \varphi_*(u\partial_u + v\partial_v)\end{cases}\,. \tag{59}$$

Therefore, we can directly compute the commutator applying the previous lemma:

$$\begin{aligned}[X, Y]_{(x,y)} &= [\varphi_* \{(\alpha u - \beta v)\partial_u + (\alpha v + \beta u)\partial_v)\}, \varphi_*(u\partial_u + v\partial_v)] = \\ &= \varphi_*[(\alpha u - \beta v)\partial_u + (\alpha v + \beta u)\partial_v), u\partial_u + v\partial_v] = \\ &= \varphi_* \begin{pmatrix} 0 \\ 0 \end{pmatrix} = \begin{pmatrix} 0 \\ 0 \end{pmatrix}.\end{aligned} \tag{60}$$

In fact, not only is Y a normalizer, but in this case also a commutator. □

This commutation relation allows us to analyze the time evolution of the gradient. We can use an analogous result to [12] (proposition 3.6).

Proposition 3.12. *Let $\phi_t(p)$ be the flow at time t generated by the field X starting at point p. If $\nabla\vartheta$ is the gradient of the asymptotic phase, it satisfies the following differential equation on the flow lines:*

$$\begin{cases} \frac{d}{dt}(\nabla\vartheta(\phi_t(x,y))) = -DX^T(\phi_t(x,y))\nabla\vartheta(\phi_t(x,y)) \\ \nabla\vartheta(\phi_0(x,y)) = \nabla\vartheta(x,y) = \beta\frac{Y^T}{X\cdot Y^T} \end{cases}. \tag{61}$$

Proof. The complete proof can be seen in appendix B of [12]. We can use the same arguments in our case because they rely on the hypothesis of the normalization relation, $[X, Y] = \mu Y$, which we showed in proposition 3.11. Note that the only difference is the normalization constant for the initial condition. This difference comes from the expression of the linearized dynamics, and only means the initial condition has to match the expression in (54). □

Equation (61) is very important; it is actually the key point to extending the PRF to a broader region. In the next sections we are going to describe how to define a fundamental domain where the error is bounded by a given tolerance. Within this region we compute Y as the pushforward of $\tilde{Y}(u, v)$, which, by (54), allows us to compute $\nabla\vartheta$. Finally, $\nabla\vartheta$ is equivalent to having a first order expression for the PRFs, but the region where this is valid is quite limited. Therefore, equation (61) is crucial to, using the previous computations as initial condition, integrate the equation backward in time and obtain $\nabla\vartheta$ outside of the domain.

3.5 PRFs on isostables

Once we have a way to compute a phase resetting functions for every point in a region of the plane around the equilibrium, we can look at the PRF as a a scalar function defined on this neighborhood. However, as in the case of limit cycles, it is more convenient and natural to look at the PRFs evaluated on closed orbits that we can parameterize by a phase. The closed curves where we are going to evaluate the PRFs are the so-called **isostables**. Isostables are sets of points that approach the focus at the same time. Like for the case of isochrons, the idea of using a simple expression in the linear space and then transfer them through the change of variable φ is useful both for the definition and the implementation. Since characterizing a set of points by saying that they approach the equilibrium at the same time is ambiguous, we are going to define the isostables in the linearized system and take the image under the change of variable to be the isostables in the nonlinear system. A more formal definition for the nonlinear case can be quite cumbersome, see

[15]. In our linear system, the idea of approaching the focus at the same time is clearly satisfied for the points in the following circles:

$$\tilde{\gamma}_r = \{(r\cos(\theta), r\sin(\theta)), \theta \in [0, 2\pi)\}\,. \tag{62}$$

Even though eventually all the points in the basis of attraction of a stable focus arrive at the equilibrium at infinite time, all the points in the isostables are at the same distance of the equilibrium. Besides, isostables are mapped to isostables by the flow:

$$\tilde{\phi}_t(\gamma_r) = \{r \cdot e^{\alpha t}\cos(\theta), r \cdot e^{\alpha t}\sin(\theta)\} = \tilde{\gamma}_{r\cdot e^{\alpha t}}\,. \tag{63}$$

Note that the isostables are now characterized by a **radius** rather than a phase. Thus, our definition of isostable is:

Definition 3.13. Given a dynamical system with a strong focus and a change of variables φ that linearizes the system, an isostable of radius r is

$$\gamma_r = \varphi(\tilde{\gamma}_r)\,, \tag{64}$$

or the image of this curve under the flow, $\phi_t(\varphi(\tilde{\gamma}_r))$.

3.6 PRCs for the linear case

Let us study what the isochrons, isostables and PRCs are like for a linear focus as a simple example. The linear system is defined by (18). Since isochrones are given by (14), the asymptotic phase is simply the angular coordinate usual polar coordinates, so:

$$\tilde{\vartheta}(u, v) = \arctan\left(\frac{v}{u}\right)\,, \tag{65}$$

so its gradient is, obviously:

$$\nabla\tilde{\vartheta}(u, v) = \left(\frac{-v}{u^2+v^2}, \frac{u}{u^2+v^2}\right)\,. \tag{66}$$

This means the PRC for an stimulus $\vec{\epsilon}$ is:

$$\mathrm{PRC}(u, v) = -\epsilon_x \frac{v}{u^2+v^2}\,. \tag{67}$$

And taking into account the linear isostables are circumferences, for a given radius r:

$$\mathrm{PRC}(\gamma_r(\theta)) = -\epsilon_x \frac{\sin(\theta)}{r}\,. \tag{68}$$

We show a plot of these objects in Figure 1.

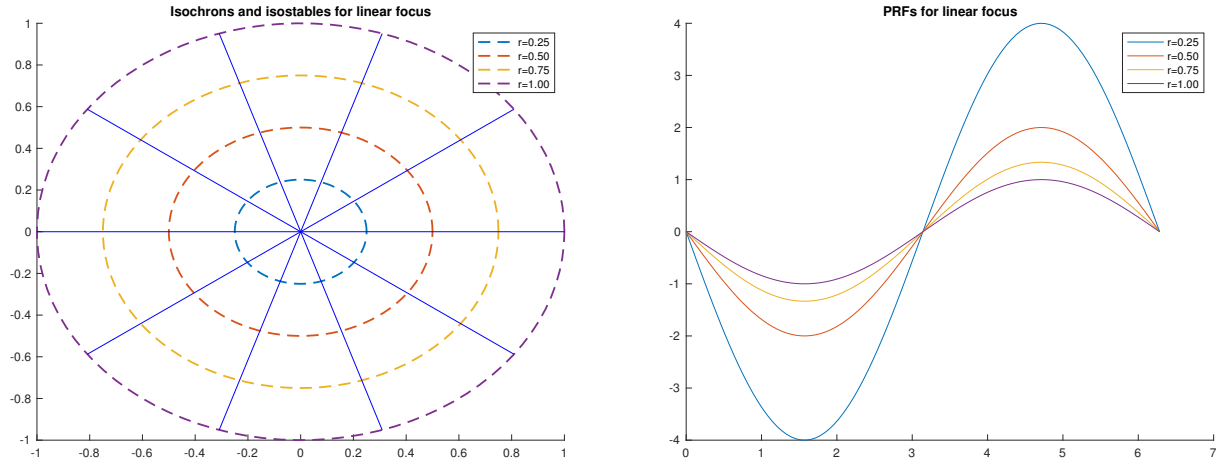

Figure 1: On the left: isostables and isochrons for a linear focus. On the right: PRCs evaluated on the corresponding isostables.

3.7 Relation with the parameterization method

The local calculation of the isochrons and isostables using a local transformation followed by an extension performed by numerical integration has already been used, see [12], to compute isochrons and phase resetting functions of limit cycles. In this case the method used for the computation of the local isochrons was the so-called **parameterization method**, developed by Xavier Cabré and Ernest Fontich as a method for computing invariant manifolds of dynamical systems. In this section we are going to briefly comment on it and its relation to the procedure we have presented. The parameterization method works in the following context: given a vector field in $\mathbb{R}^n$, $F : U \subset \mathbb{R}^n \longrightarrow \mathbb{R}^n$, which defines the dynamics, it tries to find two objects:

- **A parameterization, K, defining the d-dimensional invariant manifold** as the image of a parameter space $E \subset \mathbb{R}^n$
$$K : E \longrightarrow \mathbb{R}^n . \tag{69}$$
- **A vector field R** that expresses the dynamics in the parameter space, $R : E \longrightarrow E$.

This pair of objects has to be calculated in such a way that it fulfills **the invariance equation** that states that the dynamics can be thought of as happening in the parameter space E and then mapped to the original space by K, or as happening in the original space.

$$F \circ K = K \circ R . \tag{70}$$

That is, the following diagram commutes:

$$\begin{array}{ccc} E & \xrightarrow{K} & \mathbb{R}^n \\ \downarrow R & & \downarrow F \\ E & \xrightarrow{K} & \mathbb{R}^n \end{array} .$$

The important element of this method for the problem of computing isochrons of a limit cycle is that it contains two variables, namely, the new dynamics and the parameterization. If a specific dynamics R is fixed, then solving the equation is equivalent to finding a parameterization of the invariant manifold such that, expressed in terms of that parameterization, the dynamics are the ones we chose. On the other hand, if a specific parameterization is fixed, the invariance equation yields the form of the dynamics under that transformation. In general, if we are working on $\mathbb{R}^n$, the manifold we compute using the parameterization method is a d-dimensional manifold, that is $K(E) \subset \mathbb{R}^n$ has dimension d. However, in [12], where the systems are planar, a neighborhood of the limit cycle was parameterized, that is, the searched invariant manifold was also of dimension two. Thus, the use of this method is to express the dynamics in new variables that allow to explicitely describe asymptotic phase. In this sense, it provides a normal form for the system. Nonetheless, this expression is more flexible for the case of limit cycles, since it describes very conveniently the basin of attraction of an attractive limit cycle. Given the oscillatory condition of the limit cycle, the parameters chose where θ and σ, in such a way that θ on the limit cycle is the phase and σ accounts for displacements in the direction transversal to the limit cycle. For a planar system with a hyperbolic limit cycle with characteristic exponent λ, the parameterization method yields a parameterizing map, K, such that the dynamics for those parameters have the form:

$$\begin{cases} K : (\theta, \sigma) \longrightarrow (x, y) \\ R(\theta, \sigma) = \frac{1}{T}\frac{\partial}{\partial\theta} + \frac{\lambda}{T}\frac{\partial}{\partial\sigma} \end{cases} . \tag{71}$$

The key point for the convenience of the expression in these coordinates is that the isochrons are naturally expressed as the level curves $\gamma_{\theta_1}(\sigma) = K(\theta_1, \sigma)$ and the isostables as $\alpha_{\sigma_1}(\theta) = K(\theta, \sigma_1)$.

In the current case, since we are interested in computing the asymptotic phase near an equilibrium point, using the parameterization method for obtaining a phase-based description of the system is conceptually analogous to using a normal form to describe the neighborhood of the point. In fact, computing the normal form around the equilibrium point is the same as applying the parameterization method imposing that the dynamics are those of a linear focus, see (18).

4. Implementation

In this section we are going to explain the procedure we have followed for the numerical computation of the previously defined objects. Throughout the section we assume the system has an equilibrium of strong focus type, and that we have the change of variables φ that linearizes it. We denote by (u, v) the variables in $U \subset \mathbb{R}^2$ in which the system is linear up to order n, and $(x, y) \in V \subset \mathbb{R}^2$ the original variables.

4.1 Error treatment

Correctly analyzing and handling error is crucial for every numerical implementation. In our case we are dealing with a normal form computation, which means we are performing calculations in a space where the dynamics are simplified — in this case linear — and translating them to the original phase space via a diffeomorphism. There are several ways of evaluating the error in the computations:

- **The invariance error**: the invariance equation states that the nonlinear field applied to the variables in the nonlinear space obtained from applying the change of variables at a given point has to be

equal to the linearized change of variables, that is, the pushforward of the linear field applied at that point. It reads:

$$X(\varphi(u,v)) = \varphi_*(\tilde{X}(u,v))\,. \tag{72}$$

The equation should be exact for a complete linearization, but we can only compute a linearization of order n, so both terms differ by an error. We can estimate how correct the change is by looking at the value of the **invariance equation error**:

$$\varepsilon_{\text{inv}}(u,v) = \left|\left| X(\varphi(u,v)) - \varphi_*(\tilde{X}(u,v)) \right|\right|_2 . \tag{73}$$

Note that this equation is analogous to (70), treating φ as the parameterization and the linear focus field $\tilde{X}$ as R.

We can use this error to define the so-called **fundamental domain**, that is, the region where the invariance equation yields an error smaller than a certain tolerance. We evaluate the error for points distributed along circles of a certain radius, considering the error for that radial value to be the maximum error found at that distance. The fundamental domain is the circle inside the highest radius where the error does not exceed the tolerance:

$$\rho_{\text{fund}} = \max\{\rho \text{ such that } \max_{\theta\in[0,2\pi]}\{\epsilon_{\text{inv}}(\rho\sin(\theta),\rho\cos(\theta)) < \epsilon_{max}\}\}\,. \tag{74}$$

For our computations we have used a tolerance of $\epsilon_{max} = 10^{-9}$.

- **Orbit comparison**: another way of characterizing the error is to compare the time evolution of the linear variable to the time evolution of the nonlinear variables. For a point (u,v), we can obtain its time evolution by multiplying by the fundamental matrix, given that the linear dynamics they follow has an explicit solution:

$$\begin{pmatrix} \dot{u} \\ \dot{v} \end{pmatrix} = \begin{pmatrix} \alpha & -\beta \\ \beta & \alpha \end{pmatrix} \begin{pmatrix} u \\ v \end{pmatrix} \implies \tilde{\phi}_t \begin{pmatrix} u \\ v \end{pmatrix} = e^{t\alpha} \begin{pmatrix} \cos(\beta t) & -\sin(\beta t) \\ \sin(\beta t) & \cos(\beta t) \end{pmatrix} \begin{pmatrix} u \\ v \end{pmatrix} . \tag{75}$$

For the nonlinear system we cannot obtain the explicit flow, so we have to obtain $\phi_t(\varphi(u,v))$ using numerical integration. For the evaluation of this type of error we need to fix a time value to apply ϕ_t: we have selected a whole period in the linearized system, that is $t = \frac{2\pi}{\beta}$.

$$\varepsilon_{\text{orbit}} = \left|\left| \varphi(\tilde{\phi}_{\frac{2\pi}{\beta}}(u,v)) - \phi_{\frac{2\pi}{\beta}}(\varphi(u,v)) \right|\right|_\infty . \tag{76}$$

4.2 Computation of isochrons, isostables and phase resetting curves using the linearization

Once we have obtained a fundamental radius ρ_{fund} we can apply φ knowing the error is below the tolerance. The procedure is to compute the linear isochrons, isostables and the transversal field Y and to apply φ and φ_*. Then, we apply numerical integration to extend the results outside the fundamental domain.

4.2.1 Isochrons computation via the change of variables

The isochronous section associated to a linear strong focus are the radii $\tilde{\Sigma}_\theta = \{(r\cos(\theta), r\sin(\theta), r \in \mathbb{R}^+\}$. We split the fundamental domain in the angles $\theta_1, \theta_2, \dots, \theta_m$, so we obtain m isochrons $\tilde{\Sigma}_{\theta_i}$, $i \in (1, m)$. From these we obtain a set of m isochrons in the nonlinear system:

$$\Sigma_{\theta_i} = \varphi(\tilde{\Sigma}_{\theta_i})\,. \tag{77}$$

The flow ϕ_t maps isochrons to isochrons and it shrinks or expand them according to the attractive or repulsive character of the equilibrium. By integrating backwards in time if the equilibrium is stable and integrating forward if it is unstable, we can divide the period $\frac{2\pi}{\beta}$ by m to obtain the integration time to map an isochron to the next one, $\tau_m = \frac{2\pi}{m\beta}$. Integrating for a multiple $k\tau_m$, $k \in \mathbb{Z}$ maps isochrons as follows:

$$\phi_{k\tau_m}(\Sigma_{\theta_i}) = \Sigma_{\theta_{(i+k) \mod m}}\,. \tag{78}$$

According to the specific characteristics of the system we can vary k to maintain the numerical integration error bound by a tolerance.

4.2.2 Isostables computation via the change of variable

In the same way we split the angular length of the fundamental domain in m isochrons, we split the fundamental radius ρ in n to obtain the linear isostables $\tilde{\gamma}_{i\rho/n}$, $i \in (1, \dots, n)$. The nonlinear isostables are:

$$\gamma_{i\rho/n} = \varphi(\tilde{\gamma}_{i\rho/n})\,. \tag{79}$$

In order to extend them we follow the same procedure and integrate numerically the same time $k\tau_m$. Note that in this case an isostable is not mapped to one of the existing isostables. As mentioned in 3.5, we denote the resulting isostable in the following way:

$$\phi_{k\tau_n}(\gamma_{i\rho/n}) = \gamma_{(i\rho/n)e^{\alpha k\tau_n}}\,. \tag{80}$$

4.2.3 PRF computation using using $\nabla\vartheta$

According to (54), we can evaluate $\nabla\vartheta$ inside the fundamental domain by computing the field Y via the pushforward φ_* of the radial field Y. Given that we are interested in the PRFs evaluated on the isostables, we evaluate (54) on $\tilde{\gamma}_{r_i}$. In order to extend it outside of the fundamental domain we use 3.12. The integration time is the same $k\tau_k$ so that the result is evaluated on the extended isostables. Denoting $\psi_{k\tau_m}$ the flow of (61), we get the gradient of the asymptotic phase on the extended isostables:

$$\nabla\vartheta(\gamma_{(i\rho/n)e^{\alpha k\tau_n}}) = \psi_{k\tau_m}(\nabla\vartheta(\gamma_{i\rho/n}))\,. \tag{81}$$

Since PRFs are intended to show the intensity of a voltage stimulus on the neuron, we are only interested in the component of ϑ corresponding to V, which, in our case, is the first variable. Therefore, PRF $= \frac{\partial\vartheta}{\partial V} = \nabla\vartheta \cdot (1, 0)$

5. Results

In this section we apply the methods described previously to study two models of excitable neurons. First we comment on the models and the different dynamics that occur for various values of the parameters. Then, we compute the diffeomorphism φ and evaluate its error to obtain a fundamental domain where we can compute the isochrons and isostables as explained in 4. Finally, we compare the results for different parameters regions. We have computed the bifurcation diagrams using the software XPPAUT — see [7]. We have performed the linearization and the local computation of the isostables, isochrons and PRFs with a self-written MATLAB (The Mathworks, Natick, MA, [1]) program fixing a linearization degree of $n = 13$, and we have performed the numerical integration for extending isostables, isochrons and PRFs with a Runge-Kutta 4-5 method with adaptative stepsize and absolute tolerance $\epsilon_{max} = 10^{-15}$.

5.1 The self-excited neuron

The self-excited neuron has already been used, see [3], to study oscillatory properties of nonoscillatory neurons that interact with others or with themselves. It is in fact the symplified version of a linearized two-cell model. In this model the gating variables are lumped to a single variable, and the dynamics of membrane potential depend on this single gating variable, the leak potential and a synaptic term. In what follows the potential, V, represents the difference to the equilibrium value.

$$\begin{cases} C_i \cdot \dot{v}_i = -g_{L,i} v_i - g w - G_{syn,i} \frac{1}{1+e^{-v_j}} (v_i - E_{ex}) \\ \tau_i \dot{w}_i dt = v_i - w_i \end{cases} \quad i, j \in (1, 2) \text{ and } i \neq j \,. \tag{82}$$

In this model the synaptic conductance depends on the voltage of the other cell. However, in the self-excited neuron the synaptic current depends on the voltage of the same cell, so we can drop the indices i, j and are left with a planar system:

$$\begin{cases} C \cdot \dot{v} = -g_L v - g w - G_{syn} \frac{1}{1+e^{-v}} (v - E_{ex}) \\ \tau \cdot \dot{w} = v - w \end{cases} \,. \tag{83}$$

The set of parameters is:

- g_L: it represents the leak conductance.
- g: it represents the gated channels conductance: the higher its value the higher the impact of the gating variable w on the the system.
- G_{syn}: it stands for **synaptic conductance**, and it represents the maximum electrical conductance of the synaptic connection. The synaptic term in this case is excitatory, that is, it contributes positively to the potential balance and favours occurrence of action potentials.
- E_{ex}: it is the exciting voltage threshold of the synaptic term: when the voltage is lower than this value the contribution to the total balance is negative; the contribution is positive otherwise.
- τ: it is the gating variable **time scale**. A higher τ implies $\dot{w}$ has lower values, so w approaches v more slowly. If τ is smaller the gating variable is very fast, until it ultimately is virtually equal to the voltage v.

5.1.1 Analytic considerations

The procedure explained in the proof of Theorem 3.7 requires the field to be of polynomial form in order to express the nonlinear terms as elements of $\mathcal{H}^n$. Given that the self-excited neuron contains nonpolynomial terms, we need to express the function as a series around the critical point, which, depending on the set of parameters, will have a different value. Let us denote this equilibrium by (v^*, w^*). The first terms in the equation are straightforward since they are already in polynomial form. The part we have to find an expansion for is the synaptic strength, modeled by a **sigmoid function**, which has the following general expression:

$$\sigma(x) = \frac{1}{1 + e^{\frac{x - x_{vhlf}}{x_{slp}}}} \,. \tag{84}$$

Note the general expression contains the parameters x_{hlf} and x_{slp} that define where the function is centered and its slope, respectively. In our system, $xx_{hlf} = 0$ and $x_{slp} = 1$. In order to obtain a polynomial expression for this function we use a Taylor expansion:

$$\sigma(x) = \frac{1}{1 - e^{-x}} = \sum_{i=0}^{\infty} \frac{\sigma^i(x_0)}{i!}(x - x_0)^i \,. \tag{85}$$

For the Taylor expression we require arbitrary order derivatives of σ. We can use the following straightforward property to compute an explicit analytic expression of these derivatives that allows us to evaluate them for an arbitrary (v^*, w^*):

$$\sigma'(v) = \sigma(v)(1 - \sigma(v)) \,. \tag{86}$$

If we take higher order derivatives we obtain:

$$\begin{aligned} \sigma''(v) &= \sigma^2(1 - \sigma(v)) - \sigma(v)(1 - \sigma(v))^2 \\ \sigma^{(3)}(v) &= \sigma^3(v)(1 - \sigma(v)) - 4\sigma(v)^2(1 - \sigma(v)) + \sigma(v)(1 - \sigma(v))^2 \,. \end{aligned} \tag{87}$$

These expressions suggest a pattern of the subsequent derivatives: due to (86), we can simplify all the terms to powers of σ and $(1 - \sigma)$ and express $\sigma^n(x)$ as a finite series of those factors. We can find an iterative formula for computing the n+1-th derivative from the series expression of the n-th derivative. We write

$$\sigma^{(n)}(v) = \sum_{i=1} a_i \sigma^i (1 - \sigma(v))^{n+1-i} \,. \tag{88}$$

Taking derivatives,

$$\begin{aligned} \sigma^{(n+1)} =& \sum_{i=1}^{n} a_i i \sigma^{i-1}(1 - \sigma)\sigma(1 - \sigma)^{n+1-i} - a_i \sigma^i (n + 1 - i)(1 - \sigma)^{n-i}\sigma(1 - \sigma) = \\ =& \sum_{i=1}^{n} a_i i \sigma^i (1 - \sigma)^{n+2-i} - a_i (n - i + 1)\sigma^{i+1}(1 - \sigma)^{n+1-i} = \\ =& \sum_{i=1}^{n} a_i i \sigma^i (1 - \sigma)^{n+2-i} - \sum_{i=2}^{n+2} a_{i-1}\sigma^i (n + 2 - i)(1 - \sigma)^{n+2-i} = \\ =& a_i \sigma(1 - \sigma)^{n+1} + \sum_{i=2}^{n} (i a_i - a_{i-1}(n + 2 - i))\sigma^i (1 - \sigma)^{n+2-i} - a_n \sigma^{n+1}(1 - \sigma) \,. \end{aligned} \tag{89}$$

So, we can recursively obtain the coefficients for the next derivative:

$$\begin{cases} \tilde{a}_1 = a_1 \\ \tilde{a}_i = i a_i - a_{i-1}(n-1) \quad \text{for } 2 \leq i \leq n \\ \tilde{a}_{n+1} = -a_n \end{cases} . \tag{90}$$

The recursion in (90) gives us a polynomial that we can evaluate by replacing the value of $\sigma(v)$ for the specific v, thus obtaining the n-th derivative at that point.

We can therefore find the expansion as a polynomial vector field around the equilibrium in the following way:

1. We find the equilibrium for the first equation: equating (83) to 0 we obtain $v = w$, so the first equation in (83) becomes:

   $$-g_L v - g v - G_{syn} \frac{1}{1 + e^{-v}} (v - E_{ex}) = 0 .$$

   We solve numerically this equation using the Newton-Raphson method. Denoting by v^* our numerically obtained zero the equilibrium for the whole system is (v^*, v^*).

2. We expand the sigmoid function around the equilibrium point v^* to a certain degree n. We obtain:

   $$f(v) \approx -g_L v - g v - G_{syn} \left[\sum_{i=0}^{n} a_i (v - v^*) \right] (v - E_{ex}) . \tag{91}$$

3. Finally, we translate the equilibrium to the origin, making $\tilde{v} = v + v^*$. This has the following effect:

   $$f(\tilde{v}) \approx -g_L(\tilde{v} + v^*) - g(\tilde{v} + v^*) - G_{syn} \sum_{i=0}^{n} a_i (\tilde{v} + v^* - v^*)^i (\tilde{v} + v^* - E_{ex}) \tag{92}$$

   $$f(\tilde{v}) \approx -g_L(\tilde{v} + v^*) - g(\tilde{v} + v^*) - G_{syn} \left[\sum_{i=0}^{n} a_i \tilde{v}^i \right] (\tilde{v} + v^* - E_{ex}) . \tag{93}$$

   Rearranging the terms:

   $$\begin{aligned} f(\tilde{v}) \approx & - g_L v^* - g v^* + (v^* - E_{ex}) a_0 + [a_0 + (v^* - E) a_1 - g_L - g] \tilde{v} + \\ & + \sum_{i=2}^{n} (a_{i-1} + (v^* - E) a_i) \tilde{v}^i + a_n \tilde{v}^{n+1} . \end{aligned} \tag{94}$$

This way we express the field as a polynomial centered at $(0, 0)$. Note that, since we center the expansion around the equilibrium, the first transformation presented in the proof of 3.7 is not necessary; however, after the computations we need to restore the original coordinates by the inverse translation $v = \tilde{v} - v^*$.

5.1.2 Qualitative analysis

In order to understand what the behaviour of the system is like and what to expect from modifications of different parameters, let us discuss the impact of such modification in the excitatory and oscillatory states of

the cell. We know a passive cell does not oscillate and that, regardless of the voltage, it decays back to the equilibrium state exponentially. The oscillations in the Hodgkin-Huxley model appear thanks to the delayed action of the gating variables. **Since increasing the value of g has a positive effect on the impact of the gating variable, it favors the oscillatory behaviour**. Besides, as we have mentioned, a very high time scale makes the gating variable w be virtually equal to v, which we can interpret as decreasing the gating variable effect, thus counteracts oscillations. The opposite — **a very small timescale** —, **reinforces the gating variable and favor oscillations**.

These two parameters are common to all gated membrane models. In our case, we have another source of excitement that can push the cell to oscillate, namely the synaptic term. Since we are dealing with excitatory synapses, **an increase of the synapse conductance favours oscillations**.

As mentioned in a previous section, type II excitability is related to Hopf bifurcations whereas type I is related to SNIC. In the bifurcation diagrams we see it undergoes Hopf bifurcations when we modify the parameters g, G_{syn} or τ. Figure 2 show the Hopf bifurcation: the horizontal line represents the value of the v coordinate of the equilibrium as the parameter — shown in the x axis — varies: the red segment corresponds to attracting equilibria, whereas the black segments stands for repelling ones. As for the green dots, they represent the maximum and minimum v value of periodic orbit; the fact that they are green indicates that these orbits are attracting. Thus, we have an attractive critical point that changes its stability giving rise to an attractive periodic cycle; that is, **a supercritical Hopf bifurcation**. The scenario in the bottom left panel in Figure 2 is a little more complicated. We see the equilibrium does not change its position when the timescale changes. As we increase the value of τ two limit cycles appear: one represented by the blue dots — unstable — and the other by the green ones — stable. When the parameter keeps growing the unstable cycle decreases its radius and collapses turning the equilibrium to an unstable point. Since the limit cycle is unstable, this case is a **subcritical Hopf bifurcation**. We could summarize the behavior with respects to the parameters as follows:

- If we keep the value of $\tau = 10$ there are **no transitions to the oscillatory state**, regardless of the value of G_{syn} and g.
- For a strong enough value of the parameter τ, **an increase of the gating variable conductance, g, produces a supercritical Hopf bifurcation.**
- For a high enough value of the parameter τ, **an increase of the synaptic conductance** also results in a supercritial Hopf bifurcation.
- A decrease in the time scale of the gating variable generates, via a more complex process, a stable oscillation.

We can confirm the excitability class is II by looking at figure the bottom right panel in Figure 2. When the limit cycle appears the period is finite, so there is a lowest positive oscillation frequency and oscillations do not occur at arbitrarily low periods.

Since the transition to oscillatory state depends on the parameters g, G_{syn} and τ, it is useful to look at two-dimensional bifurcation diagrams to have a broader picture of where bifurcations occur in the parameter space. Figure 3 shows two-dimensional bifurcation diagrams for parameters $g - G_{syn}$ and $\tau - G_{syn}$. The blue line is the position of the Hopf bifurcation in the parameter space.

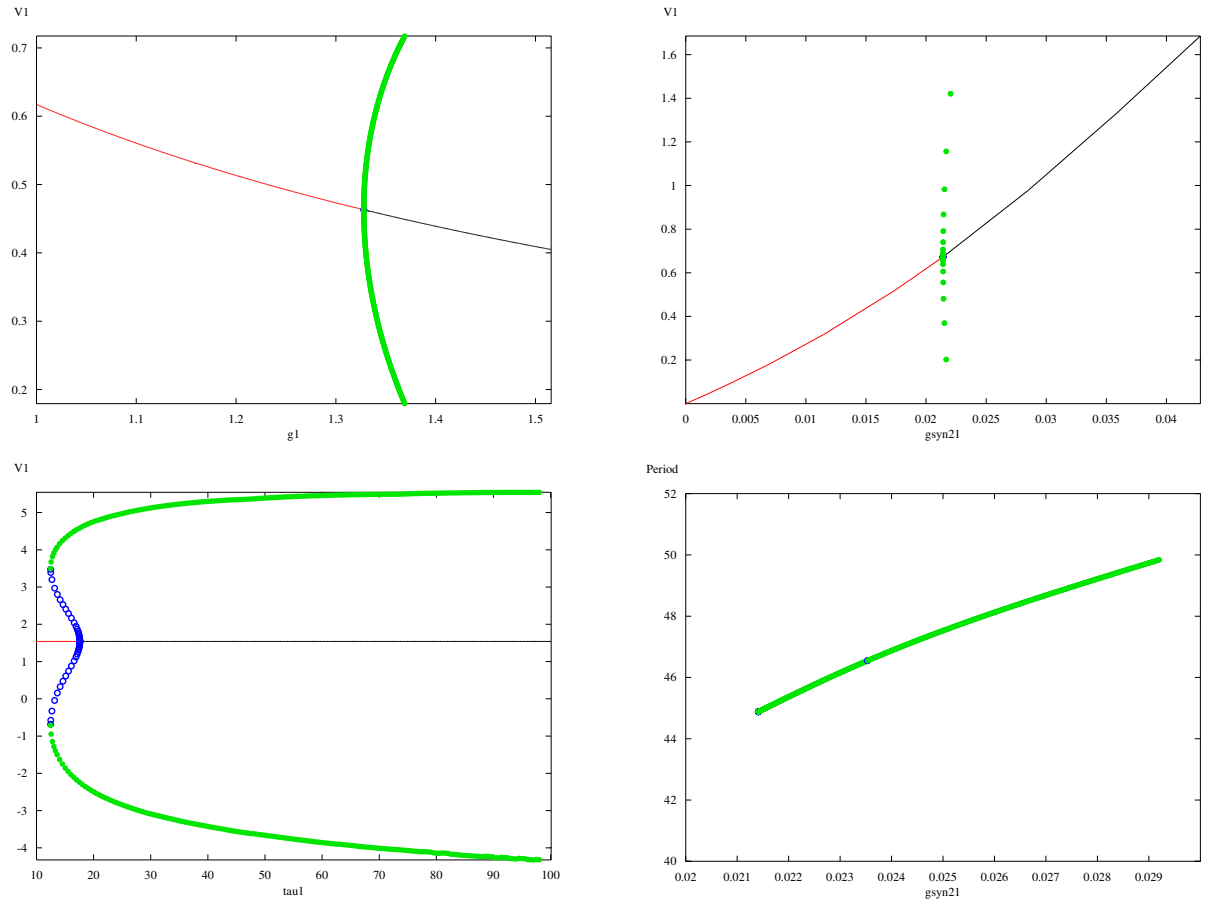

Figure 2: On the top left: bifurcation diagram for the self-excited system based on the g parameter. At $g = 1.328$ a Hopf bifurcation occurs. On the right bifurcation diagram for the self-excited system based on the maximal synaptic conductance, G_{syn}. At $G_{syn} = 0.0214$ a Hopf bifurcation occurs. On the bottom left: bifurcation diagram based on the time constant τ. In this case the Hopf bifurcation is subcritical. Before the Hopf bifurcation there is a saddle-node of limit cycle bifurcation, and a short bistability region. On the bottom right: oscillation period for the G_{syn} bifurcation above.

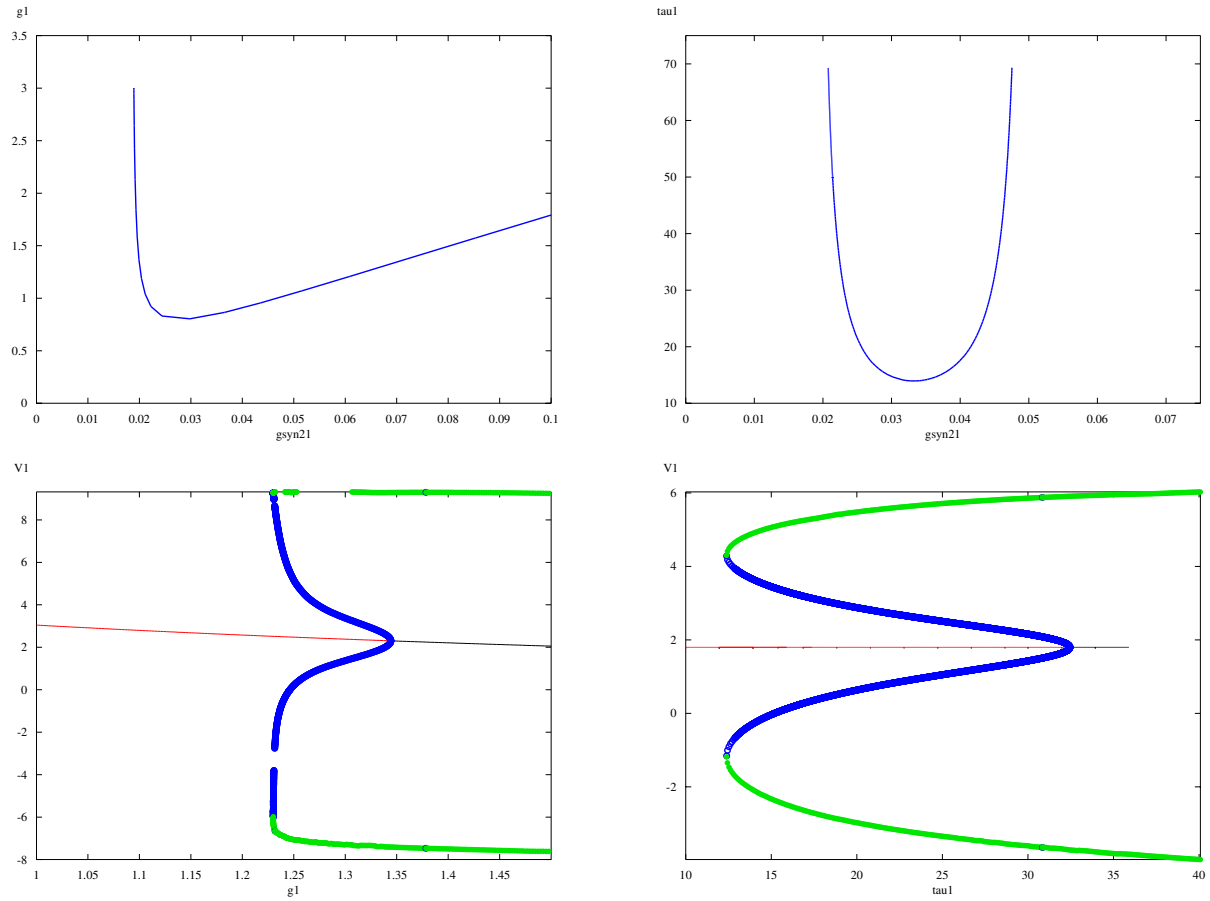

Figure 3: On the left: Hopf bifurcation for $\tau = 50$ as a function of the synaptic conductance and the gating variables conductance. On the right: Hopf bifurcation for $g = 1$ as a function of the synaptic conductance and τ. On the bottom left detail of the one parameter g bifurcation corresponding to the section of the upper left diagram where $G_{syn} = 0.07$. On the bottom right, detail of the bifurcation for the parameter τ and $G_{syn} = 0.045$

In the next section we analyze the system for different values of the parameter. First, we lookt at the low τ case without bifurcations and use it to examine the errors presented in 4.1. Then we analyze another parameter region where a bifurcation occurs. Given that the Hopf bifurcations for G_{syn} occur at very low values — $G_{syn} \approx 0.02$ — , we analyze the transitions to the oscillatory state by setting a higher value of G_{syn} and increasing g and τ. This corresponds to fixing a vertical section in the two-dimensional bifurcation diagram and moving upwards through the transition. The bottom panels of Figure 3 present the bifurcations for these sections. We see the same kind of bifurcation happens in both cases, namely one of the same type as that shown in the left bottom panel of Figure 2. Since the bifurcations are qualitatively equal we restrict our analysis to the bifurcation in τ. We split the parameter range in three regions:

1. We refer to the left part of the red segment as **monostability**: there is only one stable equilibrium point.

2. After the stable and unstable limit cycles appear there is a **bistability** region: an attractive equilibrium

point and a stable limit cycle. However, both equilibria are separated by the unstable cycle, so the transition from one to the other has to occur through a very strong stimulus.

3. We refer to the right section of the red segment as the **excitable state**: since the unstable limit cycle is very small in this region, a small stimulus will make the system transition to the oscillation.

In this section we present the results for different sets of parameters: and a case where we approach a Hopf bifurcation by increasing the time constant for a constant synaptic conductance.

5.1.3 Low τ and high synaptic conductance

In this section we have used the following paramenters:

- $g_L = 0.25$,
- $G_{syn} = 0.06$,
- $C = 1$,
- $\tau = 10$,
- $g = 1$,
- $E_{ex} = 60$.

Since the τ is 10 there is no bifurcation. This region of parameters provides damped oscillations, so the cell is in an excitable state. We use this case also as the context to illustrate the error behavior.

Effect of the linearization degree

We compute the aforementioned **orbit error** and **invariance equation** error in a neighbourhood of the equilibrium. Even though we use an approximated polynomial vector field for the computation of the linearization, we use the exact equation for the computation of the orbits and the invariance equation. In Figure 4 we show the radial orbit and invariance equation errors for several linearization degrees. Note how the increasing linearization keeps the error at a lower rate for a longer radius, though it makes the slope higher when it starts to grow.

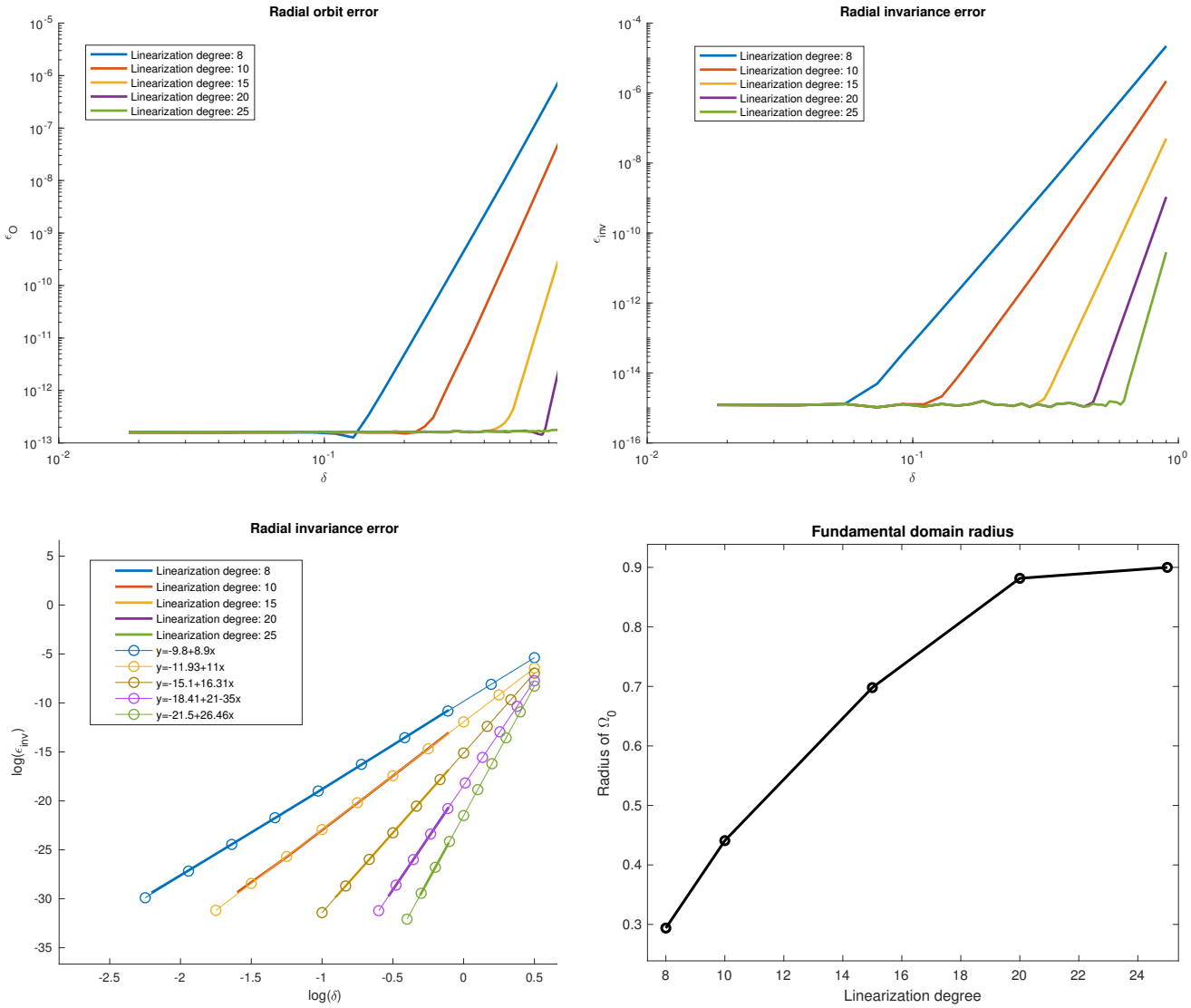

Figure 4: On the top left: radial orbit error for linearization degrees 8, 10, 15, 20 and 25. On the top right: invariance equation error for the same degrees. Both pictures are displayed in logarithmic scale for both axes. On the bottom left: radial invariance error with linear fitting for linearization degrees 8, 10, 15, 20, 25. On the bottom right: Fundamental domain radius around equilibrium equation as a function of the linearization degree.

We can examine more precisely the dependence on the linearization degree by computing linear regression of the logarithm of the data. Indeed, if we plot the logarithm of the error with respect to the logarithm of the radius, we see in equation (95) the slope is the exponent of the independent variable. We show the linear regressions in Figure 4. Observe the error grows with the $k+1$ power of the radius, which is in accordance with chapter 2 of [13]. On the right of the same picture 4 we see the increase of the linearization degree also increases the fundamental domain radius.

$$\log(\epsilon_{inv}) = (k+1)\log(\delta) + C \implies \epsilon_{inv} \approx \tilde{C}\delta^{k+1}\,. \tag{95}$$

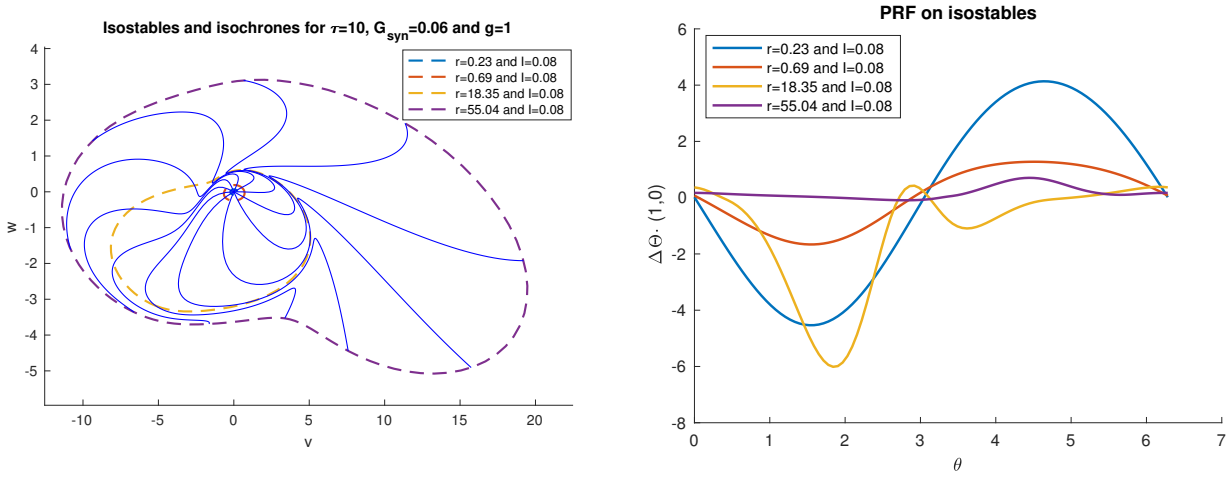

Figure 5: On the left: in blue isochrons, in red local isostables and in green extended isostables. On the right PRFs computed on the extended isochrons. The parameters are $\tau = 10$, $G_{syn} = 0.06$ and $g = 1$.

Finally, Figure 5 presents the extended isochrons, the isostables and the PRFs on those isostables for the self-excited system with $\tau = 10$, $g = 1$ and $G_{syn} = 0.06$. We see the blue PRC — $r = 0.23$ — is very similar to the linear focus PRCs (Figure 1) and reaches high values, given that it is very close to the equilibrium. As we move away from the equilibrium the values of the PRCs decrease, with exception of the regions where the isochrons are very close to one another, like the yellow isostable — $r = 18.35$. For this isostable there is a negative peak, since for very close isochrons, any stimulus has a dramatic effect on the phase. The PRCs shapes is distorted from the linear according to the geometry of the isostables.

5.1.4 The bifurcation on τ

We now analyze the bifurcation in the bottom right panel of Figure 3: we fix $G_{syn} = 0.045$ and take $\tau = \mathbf{10.32}$ **for the monostability region**, $\tau = \mathbf{22}$ **for the bistability region**, and $\tau = \mathbf{32}$ **for the excitable regime**. The rest of the parameters remain unchanged:

- $g_L = 0.25$,
- $C = 1$,
- $g = 1$,
- $E_{ex} = 60$;.

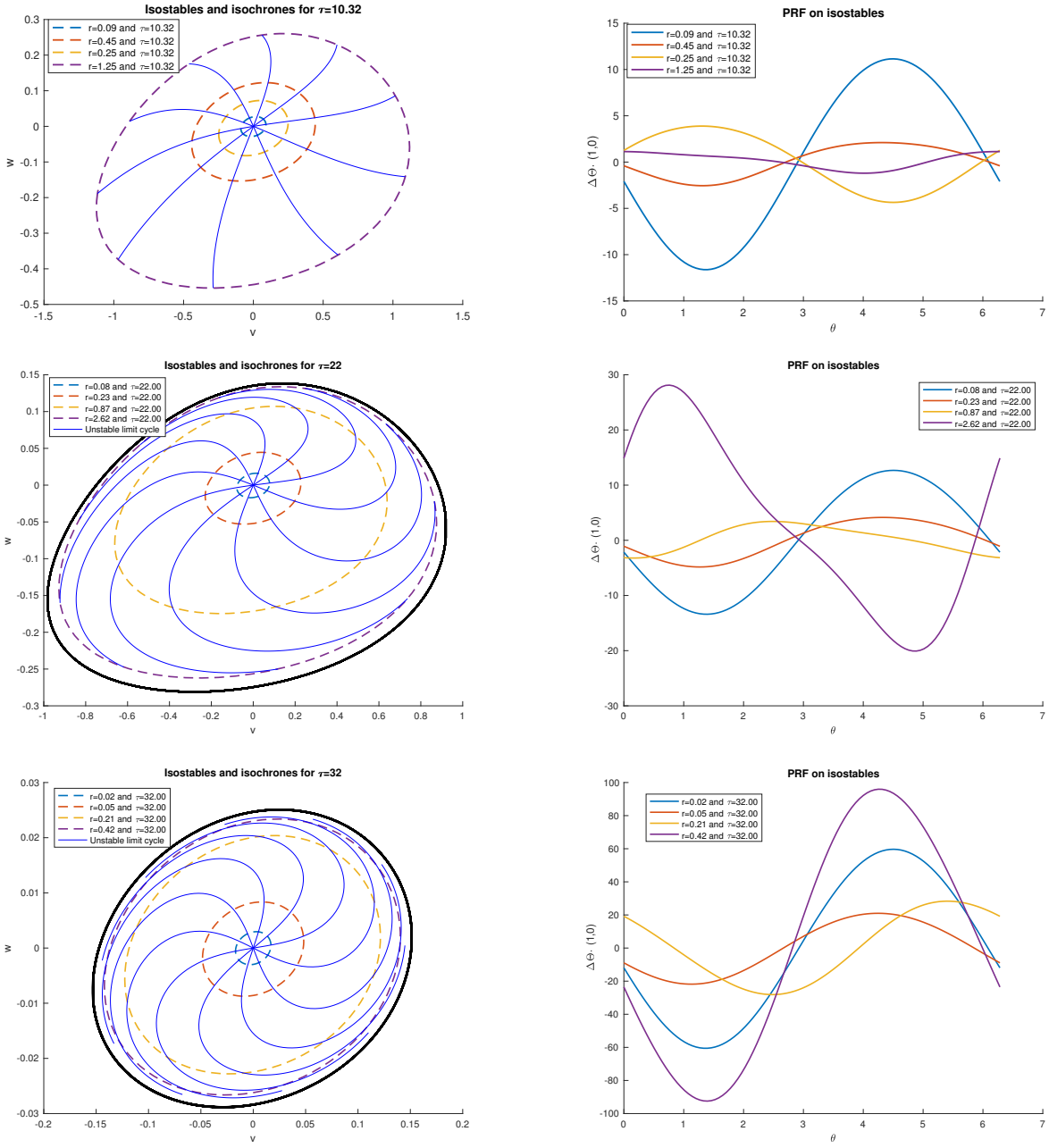

Figure 6: The three rows represent three sets of parameters differing by the value of τ. The rest of the parameters are $g_L = 0.25$, $G_{syn} = 0.045$, $C = 1$, $\tau = 32$, $g = 1$, $E_syn = 60$. The first row is for $\tau = 10.32$, the second for $\tau = 22$ and the third for $\tau = 32$. These values correspond to three regions in the bifurcation diagram in Figure 3: the region with one attractor, the bistability region and the excitable state near the Hopf bifurcation.

In Figure 6 we observe that for the value $\tau = 10$, where there is only one attractor, the PRCs are of type I and decrease with the radius. Since the isochrons acumulate close to the singular point, the equilibrium is a singularity of the phase function, so it makes sense for it to decrease with the distance. However, when

we look at $\tau = 22$ and $\tau = 32$ we see that the PRCs decrease for the first two isostables as they get farther from the equilibrium, but they increase again close to the unstable limit cycle. We can understand this by noting that the limit cycle is another singularity for the phase, given that isochrons get infinitely close as they spiral around the limit cycle. Thus, we can say that the emergence of the limit cycle does not have an effect on the shape of the PRC, but on how its intensity varies. Furthermore, there is no remarkable qualitative difference for the values $\tau = 22$ and $\tau = 32$, so the Hopf bifurcation does not have any other effect than to reduce the region where the isochrons are defined as a result of the shrinking of the limit cycle.

5.2 Fitz-Nagumo model

5.2.1 Qualitative analysis

The Fitzhugh-Nagumo equation is a classical model for oscillatory systems, and it has the following form:

$$\begin{cases} \dot{v} = v(v-a)(1-v) - w + I_{app} \\ \dot{w} = \epsilon(v - \gamma w) \end{cases} . \tag{96}$$

As usual, v is the membrane potential and w can be thought of as a simplified gating variable. In the case of the self-excited neuron we saw it went through a subcritial Hopf bifurcation. We are going to use the Fitzhugh Nagumo model to study the case of a supercritical bifurcation, which we can obtain using the following parameters:

- $a = 0.1$,
- $\epsilon = 0.1$,
- $\gamma = 1$,
- I_{app}: it is the intensity applied to the system, Increasing this parameter is what induces the supercritical Hopf bifurcation. We vary I_{app} in the range $(0.8, 0.15)$.

Unlike the case of the self-excited neuron, the system is already a third degree polynomial, so we do not need to perform any further changes to adapt it for the algorithm. We want to observe the supercritial Hopf bifurcation; but this system can have more types of behaviour. The important parameter to ensure that increasing the intensity I_{app} results in a supercritical Hopf bifurcation is γ. We can study analytically the equilibria of the system:

$$\begin{cases} v(v-a)(1-v) - w + I = 0 \\ \epsilon(v - \gamma w) = 0 \implies v = \gamma w \end{cases} \implies I = w - v(v-a)(1-v)\,. \tag{97}$$

This equation, which is a cubic, is a curve where the values of I produce equilibria. For the right range of parameters this cubic can have a maximum and a minimum. In this case, if the I_{app} approached the minimum from below, reaching the minimum value would generate an equilibrium point, and likewise approaching the maximum from above. Thus, there would be two bifurcation points where two equilibria would collide, that is, we would have a saddle-node bifurcation. In order for equation (97) to have two

local extrema we need its derivative to have two zeros, so the discriminant of the quadratic equation has to be positive:

$$\Delta \frac{d}{dv} I_{app}(v) = \Delta(3v^2 - 2(1+a)v + \left(a + \frac{1}{\gamma}\right)) > 0$$
$$4(1+a)^2 - 12\left(a + \frac{1}{\gamma}\right) > 0 \implies \gamma > \frac{3}{1 - a + a^2}\,. \tag{98}$$

For our choice of $a = 0.1$ we would therfore need $\gamma > 3.29$. We summarize the two kinds of bifurcations in Figure 7.

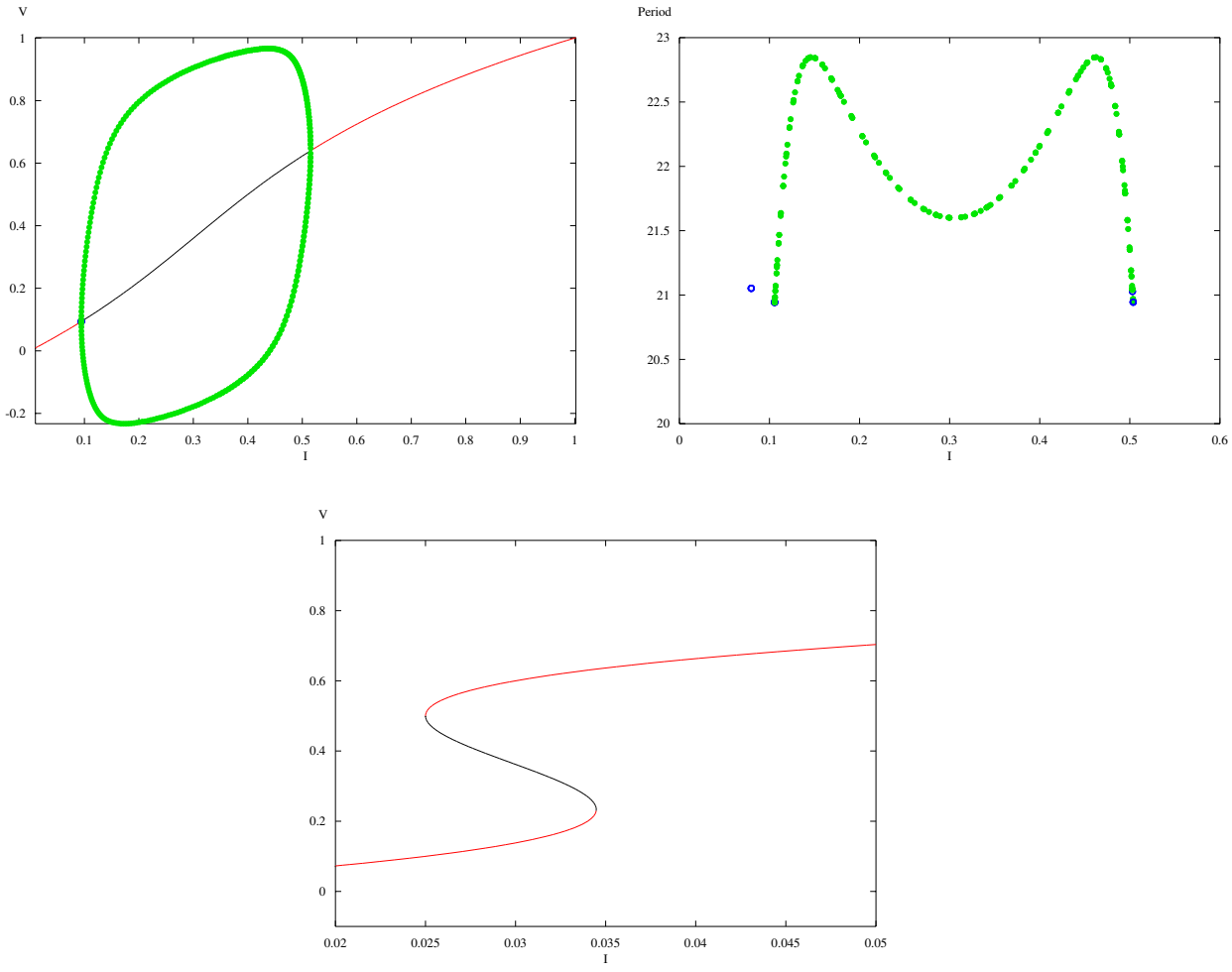

Figure 7: Bifurcation diagram for the parameter I_{app}. The rest of the parameters have values: $a = 0.1$, $\epsilon = 0.1$, $\gamma = 1$. Bifurcation occurs at $I_{app} = 0.106$. Bottom: two saddle-node bifurcations for $\gamma = 4$. Bifurcations occur at 0.025 and 0.3448.

We analyze the bifurcation shown in the top left panel of 7 distinguishing two regions:

1. The left part of the red segment is the **excitable state**. There is only one stable equilibrium.

2. The black segment defines the **oscillatory regime**: the equilibrium loses stability and a stable limit cycle emerges.

5.2.2 Excitable state

For the excitable state we take two I_{app} values: $\mathbf{I_{app} = 0.08}$ — further from the bifurcation — and $\mathbf{I_{app} = 0.1}$ — closer to the bifurcation.

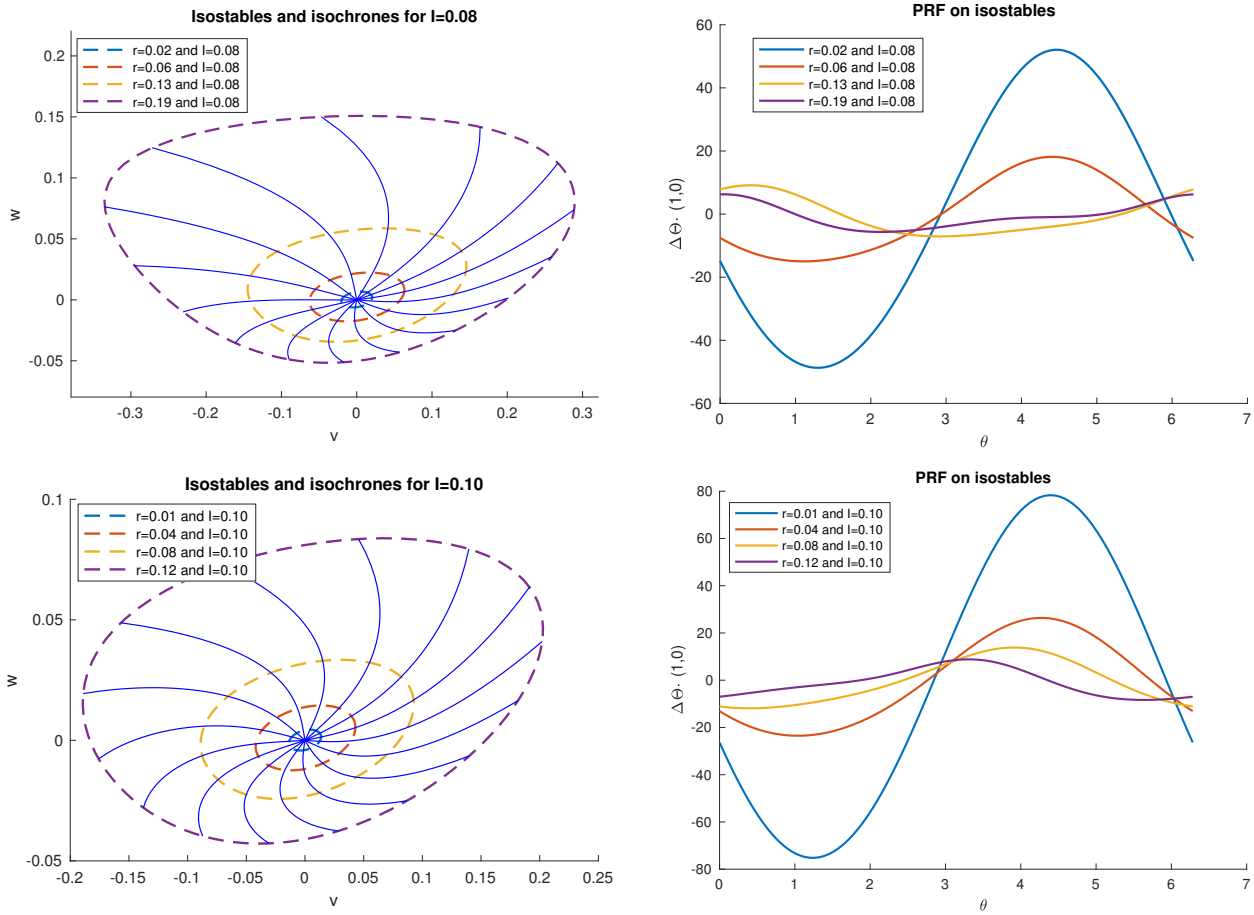

Figure 8: Isochrons, isostables and PRFs for the excitable region. The upper row contains plots for a more distant point to the bifurcation, whereas the second one shows the results for an intensity very close to the bifurcation value, $I_{app} = 0.106$. On the left: isochrons and four isostables. On the right: the PRC for the corresponding isostables. The rest of the parameters are the above mentioned: $a = 0.1$, $\epsilon = 0.1$ and $\gamma = 1$.

In Figure 8 we see the behaviour is very similar to the self-excited neuron in the monostability case: the isochrons are radial and the phase is very sensitive to impulses near the equilibrium point whereas this sensitivity decreases with the distance. We see in the blue PRFs — $r = 0.02$ and $r = 0.01$, respectively — that very near the focus the shape is almost exactly that of the PRFs for a linear focus (Figure 1). As we move away from the equilibrium, the type 1 character of the PRF is maintained, but the shape is distorted

depending on the geometry of the orbits.

5.2.3 Oscillatory state

For the oscillatory state we also use two I_{app} values: $\mathbf{I_{app} = 0.11}$ — closer to the bifurcation — and one further from it — $\mathbf{I_{app} = 0.12}$.

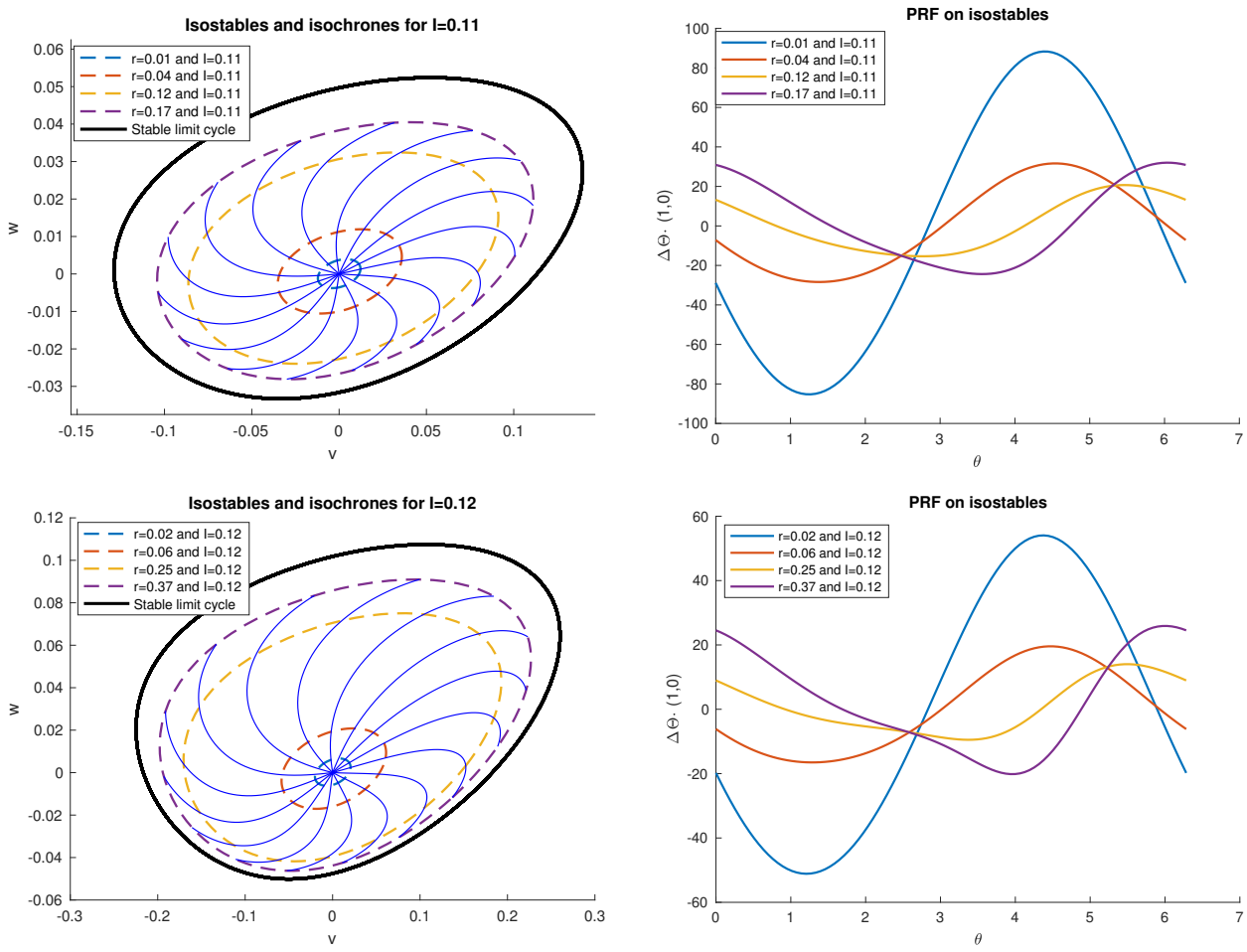

Figure 9: Isochrons, isostables and PRFs for the oscillatory. The upper row contains plots for a close point to the bifurcation, and the second for a more distant value. On the left: isochrons and four isostables. On the right: the PRC for the corresponding isostables. The rest of the parameters are the above mentioned: $a = 0.1$, $\epsilon = 0.1$ and $\gamma = 1$. The black solid thicker line represents the stable limit cycle.

In Figure 9 we see that the effect of the supercritical Hopf bifurcation on the behaviour of PRFs is very similar to the subcritical case: the emergence of a stable limit cycle delimits a region where the isochrons spiral together, causing them to get closer. As before, the blue PRFs — $r = 0.01$ and $r = 0.02$, respectively — have the same shape as PRFs of linear foci and very high values due to the proximity to the equilibrium. As we move away from the equilibrium the type I character is maintained but the shape is distorted. The values decrease for the orange PRCs — $r = 0.04$ and $r = 0.06$ —, but we observe, unlike the case where

there is no limit cycle, it increases again between the yellow and the purple ones — $r = 0.12$ and $r = 0.17$ for the top plot and $r = 0.25$ and $r = 0.37$ for the bottom plot. Finally, we see no qualitative difference between the two values of I_{app}.

6. Conclusion

In the first sections we have reviewed the concepts of phase, asymptotic phase, isochrons and phase resetting curves and have reviewed theoretical results that have allowed us to extend them rigurously to cases beyond oscillatory systems with limit cycles. We have adapted some techniques in [12] for the excitable case, identifying what methods were also valid in our case. We have used the simplest approach to computing isochrons and asymptotic phase, namely performing a linearization up to a certain degree n. We have analyzed the hypotheses needed for this linearization to be possible and describing in detail how to procede in the calculations. The use of this approach has been successful for the local computation of isochrons and asymptotic phase, as the error analyses show. We have restricted the study to strong foci, since excitable cells are generally represented by this kind of equilibria. However, from a theoretical point of view it could be of interest to examine in more detail the case of weak foci, where the real part of the eigenvalues is zero.

In the last part we have applied the methods to two particular systems, namely the self-excited neuron and the Fitzhugh Nagumo. We have been able to see how changes in the dynamics such as Hopf bifurcation and other ways of generating stable limit cycles affect the phase resetting curves. The general behaviour is that the PRFs reach very high values and have almost a perfect sinusoidal form near the equilibrium, and they reach lower values and present irregular shapes that depend on the geometry of the isostables as we move away from it. However, when there is a limit cycle surrounding the equilibrium, the isochrons tend to spiral towards it and the PRFs reach very high values in their vicinity. Even though the existence of a limit cycle does have an impact on the PRFs — making them increase as the isostables approach the cycle — it seems that the type of bifurcation that generates the limit cycle does not have a visible effect.

In this context, it would have been interesting to extend the results not only to the effect of stimuli on the phase of a point, but also the effect the stimulus has in shifting a point from an isostable to another. These calculations could follow the theory developed in [5], and essentially would the analogous to the calculation of PRFs using, instead of Y, a different vector field — referred to as Z in [5].

A further interesting study would be how the phase resetting of excitable cells could relate to their phase resetting when they are in a network and produce oscillations. This task, however, has proved harder than expected given that networks of cells are higher dimensional systems and the method we have worked with is only suitable for two-dimensional systems. However, this problem could be tackled by computing the phase resetting curves of the separate cells using planar methods and *numerically stimulating* the perturbation of the network to extract directly the phase resetting functions for the network system.

Finally, a more detailed study of oscillatory systems and their phase and amplitude response could provide information on the intensity and the time when we should stimulate the system in order to force oscillations and prevent it from falling back to the equilibrium. This, however, requires a more detailed analysis and was outside the scope of this work.

References

[1] MATLAB, R2018b, 2019.

[2] A. Algaba and M. Reyes. Characterizing isochronous points and computing isochronous sections. *Journal of Mathematical Analysis and Applications*.

[3] Andrea Bel and Horacio G. Rotstein. Membrane potential resonance in non-oscillatory neurons interacts with synaptic connectivity to produce network oscillations.

[4] Xavier Cabré, Ernest Fontich, and Rafael de la Llave. The parameterization method for invariant manifolds iii: overview and applications. 2004.

[5] Oriol Castejón, Antoni Guillamon, and Gemma Huguet. Phase-amplitude response functions for transient-state stimuli. 2013.

[6] G. Barc Ermentrout. *Simulating, Analyzing, and Animating Dynamical Systems: A Guide to XPPAUT for Researchers and Students (Software, Environments and Tools)*. Society for Industrial and Applied Mathematics, 1987.

[7] G. Bard Ermentrout. XPPAUT 8.0, 2016. `http://www.math.pitt.edu/~bard/xpp/xpp.html`.

[8] Terman David H. Ermentrout, G. Bard. *Mathematical foundations of neuroscience*. Springer, 2010.

[9] X. Cabré et al. The parameterization method for invariant manifolds iii: overview and applications. *Journal of Differential Equations*.

[10] Jaume Giné and Maite Grau. Characterization of isochronous foci for planar analytic differential systems. *Proceedings of the Royal Society of Edinburgh, 135A*.

[11] John Guckenheimer and P. J. Holmes. *Nonlinear Oscillations, Dynamical Systems, and Bifurcations of Vector Fields*. Springer, 1983.

[12] Antoni Guillamon and Gemma Huguet. A computational and geometric approach to phase resetting curves and surfaces. *Journal of Mathematical Analysis and Applications*.

[13] À. Haro, M. Canadell, J.-Ll. Figueras, A. Luque, and J.M. Mondelo. *The parameterization method for invariant manifolds: from rigorous results to effective computations*. Springer, 2016.

[14] Eugene M. Izhikevich. *Dynamical Systems in Neuroscience*. 2007.

[15] A. Mauroy, I. Mezić, and J. Moehlis. Isostables, isochrons, and Koopman spectrum for the action–angle representation of stable fixed point dynamics. 2013.

[16] M. Sabatini. Isochronous sections via normalizers.